PART IV:

NICMOS

- NICMOS

Chapter 14
NICMOS Instrument Overview

In This Chapter...

This chapter presents a brief overview of the Near Infrared Camera and Multi-Object Spectrometer (NICMOS) instrument capabilities, its readout modes, and data products.

14.1 Instrument Overview

NICMOS was built by Ball Aerospace Corporation for the University of Arizona, under the direction of Rodger I. Thompson, the Principal Investigator. A basic description of the instrument and its on-orbit performance through the Servicing Mission Orbital Verification program is provided by Thompson et. al (1998).[1] We encourage all NICMOS users to reference this paper and to review the related papers in the special *ApJ Letters* which describe the Early Release Observations and demonstrate the scientific capabilities of NICMOS.

NICMOS provides imaging capabilities in broad, medium, and narrow band filters, broad-band imaging polarimetry, coronographic imaging, and slitless grism spectroscopy, in the wavelength range 0.8–2.5 μm. NICMOS is an axial instrument and has three adjacent but not contiguous cameras, designed to operate independently and simultaneously. Each camera has a different magnification scale, and is equipped with a dedicated 256 x 256 HgCdTe Rockwell array. The pixel size and field of view are 0”.043 and 11”x11” in Camera 1 (referred to as

1. Thompson, R.I., M. Rieke, G. Schneider, D.C. Hines, and M.R. Corbin, 1998, *ApJL*, 492, L95.

NIC1), 0”.075 and 19”.2x19”.2 in NIC2, and 0”.2 and 51”.2x51”.2 in NIC3. Information about detector performance can be found in the *NICMOS Instrument Handbook* and at the NICMOS WWW page:

```
http://www.stsci.edu/ftp/instrument_news/NICMOS/
topnicmos.html
```

Each camera is provided with its own set of filters, mounted on three independent wheels. There is a total of 20 filter positions on each wheel, of which one is BLANK and three of the others are occupied by either polarizers or grisms. The remaining 16 positions of each filter wheel are occupied by broad, medium, and narrow band filters. The list of these filters is given in the *NICMOS Instrument Handbook*. The filters (including polarizers and grisms) cannot be crossed with each other, and are used as single optical elements.

NIC1 and NIC2 each contain three polarizers, whose principal axes of transmission are separated by 120 degrees. The spectral coverage is fixed for each camera. The polarizers cover the wavelength range 0.8–1.3 μm in NIC1, and 1.9-2.1 μm in NIC2. Observations in the three polarizers of each camera are used to derive the Stokes parameters of linearly polarized light.

The filter wheel of NIC3 contains three grisms which can be used to perform slitless spectroscopy in the wavelength range 0.8–2.5 μm. The three grisms cover the range 0.8–1.2 μm, 1.1–1.9 μm, and 1.4–2.5 μm, respectively.

In NIC2, a coronographic spot is imaged onto the focal plane and provides a circular occulted region of 0”.3 in radius (with a useful effective radius of 0”.4). For coronographic imaging, an acquisition sequence is required at the beginning of the observation to center the target under the occulting spot.

Each 256 x 256 detector array is divided into four 128 x 128 quadrants, each of which is read out by an amplifier at the corner of the quadrant. There are four amplifiers in each camera. Unlike CCDs, infrared array pixels are read independently, implying that problems like charge transfer efficiency or bleeding are not present. The three cameras operate independently, implying that optical elements, integration times, and readout modes can be different in each.

14.2 Detector Readout Modes

NICMOS does not have a physical shutter mechanism, and exposures are obtained through a sequence of reset and read operations. In particular, a typical exposure will be the product of the following steps:

1. ***Array reset***: the pixels are set to the bias level.
2. ***Array read***: the charge in each pixel is measured and stored in the on-board computer’s memory. This read is performed immediately after the reset, and contains the reference level for the exposure (zeroth read). In practice, the readout is performed 0.203 seconds after the reset, implying that it represents a finite, though very short, exposure. This readout is performed non-destructively—the charge in each pixel is left intact.

3. ***Integration***: NICMOS integrates for the user-specified time.
4. ***Array read***: the charge in each pixel is measured and stored in the on-board computer's memory. Again, the readout is non-destructive.

The beginning of an integration is marked by the zeroth read, which is always preceded by a reset. Since all readouts are non-destructive, namely, do not change the value of the charge accumulated on the pixel, the last two steps of the sequence above can be repeated multiple times, and the last read of the sequence will be called the *final read*. The total integration time of an exposure is defined as the time between the final and the zeroth read of the first pixel in the array. The scientific image is given by the difference between the final and the zeroth readouts. Four readout modes have been defined for NICMOS, exploiting the flexibility allowed by the non-destructive reads:

- MULTIACCUM.
- ACCUM.
- BRIGHTOBJ.
- RAMP.

Each mode is described in the following sections, with larger emphasis on MULTIACCUM, which is by far the most used and best calibrated mode.

14.2.1 MULTIACCUM

In a MULTIACCUM (MULTIple ACCUMulate) exposure, the zeroth read is followed by several other non-destructive readouts during the course of a single integration. All of the readouts are stored in the on-board computer's memory and sent to the ground. Because the readouts are non-destructive, accumulated counts are built up from one readout to the next, with the last readout containing the accumulated counts from the entire integration time of the observation. In an exposure, the number of readouts after the zeroth and the temporal spacing between each read is selected by the user from a set of 16 pre-defined SEQUENCES. The user specifies the number of readouts through the NSAMP keyword during the Phase II. NSAMP+1 (including the zeroth read) images will be returned to the ground. For NICMOS the maximum value of NSAMP is 25 in each sequence (for a total of 26 images returned to the ground).

Since MULTIACCUM gives information not only at the beginning and at the end of an exposure, but also at intermediate times, it is the mode of choice for the vast majority of astronomical observations, from objects with large dynamical range to deep field integrations. The intermediate reads can also be used to remove the effects of cosmic ray hits and of saturated pixels from the final processed image.

The images returned to the ground by the MULTIACCUM readout are *raw* detector readouts, since not even the bias level (the zeroth read) is subtracted. This operation is performed by the ground calibration pipeline.

14.2.2 ACCUM

ACCUM is a simplified version of MULTIACCUM: the zeroth read is followed by one read (the final readout) after an amount of time specified by the integration time. The difference between the final and the zeroth readouts is computed on board, and the resulting image is sent to the ground. In this form, the ACCUM mode produces data very similar to the more familiar CCD images. A variation to this basic operation is available, which replaces the single initial and final readouts with multiple (initial and final) readouts. After the initial reset pass, *n* non-destructive reads of the detector immediately follow, as close together in time as allowed by the detector electronics. The average of the *n* values is stored as the initial value for each pixel. At the end of the integration, there are again *n* non-destructive readouts with the final value for each pixel being the average of the *n* reads. The number *n* of initial and final reads is specified by the observer and is recorded in the value of the NREAD (number of reads) header keyword in the science data files. The returned image is the difference between the averaged final and initial values. The integration time is defined as the time between the first read of the first pixel in the initial *n* passes and the first read of the first pixel in the final *n* passes. The advantage of the multiple initial and final (MIF) readout method is that, in theory, the read noise associated with the initial and final reads should be reduced by a factor of sqrt(*n*), where *n* is the number of reads. The currently supported NREAD values are 1 and 9.

14.2.3 BRIGHTOBJ

The BRIGHTOBJ (BRIGHT OBJect) mode provides a way to observe objects that would usually saturate the detector in less than the minimum available exposure time (which is the amount of time it takes to read out the array and is 0.203 seconds). In BRIGHTOBJ mode each individual pixel (per quadrant) is successively reset, read, integrated for a time requested by the observer, and read again, and then these steps are performed for the next pixel in the quadrant. The returned image contains the number of counts accumulated between the initial and final reads for each pixel (just like ACCUM mode). Since each quadrant contains 16,384 pixels, the total elapsed time to take an image in this mode is 16,384 times the requested exposure time for each pixel.

This readout mode has proven difficult to use because of the non-linearity of the detector in the presence of bright targets, even for very short exposure times.

14.2.4 RAMP

RAMP mode makes multiple non-destructive reads during the course of a single exposure much like MULTIACCUM, but only a single image is sent to the ground. The RAMP mode divides the total integration time *T* into *n* equal intervals $t = T / n$. Each readout is differenced (on-board) with the previous readout and used to compute a running mean of the number of counts (per sample interval) and an associated variance for each pixel. Large deviations from the running mean are used to detect saturation or a cosmic ray hit. At the end of the exposure, the data sent to the ground comprise a mean countrate image, plus the variance and the number of valid samples used to compute each pixel value. The effective exposure time for the returned image is the sample interval *t*.

Although this mode could be used in principle to obtain the same benefit of a MULTIACCUM exposure without the large data volume, the difficulty of implementing infallible algorithms for the cosmic ray rejection has made this mode of secondary use relative to MULTIACCUM.

Chapter 15
NICMOS Data Structures

In This Chapter...

This chapter is a guide to the structure of NICMOS data. The data file naming convention, formats, and organization are described, as are the file header keywords. The connection between the Phase II exposure logsheets and the data you receive is also explained, together with the paper products delivered.

15.1 NICMOS Data Files

STScI automatically processes and calibrates all NICMOS data and archives the data files resulting from pipeline processing in FITS format. If you have retrieved NICMOS files from the Archive (see Chapter 1), you will notice that their names look like this:

*n3w2a1wqm*_cal.fits

The first part of the file name (n3w2a1wqm) is the *rootname*, identifying the dataset to which the file belongs, the second (cal) is the *suffix*, identifying the type of data the file contains, and the third (fits) indicates that this is a FITS format file. Chapter 2 shows how to access the data contained in NICMOS FITS files; Appendix B explains how to decipher the rootnames of these files and explains why some of them are grouped into data *associations*. This section describes the different types of files that constitute a NICMOS dataset.

15.1.1 File Name Suffixes

Each file in a NICMOS dataset has a three-character suffix that uniquely identifies the file contents. Table 15.1 lists the file name suffixes for NICMOS and the corresponding file contents. The files that contain final calibrated data (which you will most likely use for analysis) are highlighted. This table lists *all* of the files that the pipeline *can* produce. For some observing strategies not all of the processing steps are performed and only a subset of these files will be produced by the pipeline. A brief explanation of the contents and origin of each file is given below.

- *Raw Science File* (`_raw`):
  This FITS file contains the raw image data received from the spacecraft. One file per exposure is created (a MULTIACCUM exposure is considered a single exposure irrespective of the number of samples specified).
- *Support File* (`_spt`):
  This FITS file contains supporting information about the observation, the spacecraft telemetry and engineering data from the instrument that was recorded at the time of the observation.
- *Association Table* (`_asn`):
  This file is a FITS binary table that contains the list of datasets making up an association.
- *Calibrated Science File* (`_cal`):
  This FITS file contains the calibrated science data for an *individual dataset*, and is produced by the pipeline calibration task **calnica** (see Chapter 16). The input to **calnica** are the `_raw` images. For a MULTIACCUM exposure, this file contains a single science image formed by combining the data from all samples.
- *Intermediate Multiaccum Science File* (`_ima`):
  This FITS file is also produced by the pipeline task **calnica** and contains the calibrated science data for all samples of a MULTIACCUM dataset before the process of combining the individual readouts into a single image has occured. This file is only produced for MULTIACCUM observations.
- *Mosaic Files* (`_mos`):
  These FITS files contain the composite target and, for chopped pattern sequences, background region images constructed by the pipeline task **calnicb** for an associated set of observations (see Chapter 16). The inputs to **calnicb** are the calibrated `_cal` images from **calnica**. Target images are co-added and background-subtracted. The value of the last character of the rootname is 0 for targets, and 1 to 8 for background images. These files are only produced for an associated set of observations.
- *Post-calibration Association Table* (`_asc`):
  This table is produced by the pipeline calibration task **calnicb,** and **is** the same as the association table _asn, with the addition of new columns which report the offsets between different images of the mosaic or chop pattern as calculated by the pipeline, and the background levels computed for each image. This file is only produced for an associated set of observations.

- *Trailer File*:
  This file contains a log of the pipeline calibration processing that was performed on individual datasets and mosaic products.
- *Processing Data Quality File* (_pdq):
  This FITS ASCII table provides quality information on the observation, mostly on pointing and guide star lock. Possible problems encountered, e.g., a loss of guide star lock or a guide star acquisition failure, are reported here.

Table 15.1: NICMOS File Name Suffixes

Suffix	File Contents
	Raw Data Files
_raw	Raw science data
_spt	Support file containing Standard Header Packet and Unique Data Log information
_asn	Association table
	Calibrated Data Files
_cal	Calibrated science data
_ima	Intermediate multiaccum calibrated science data
_mos	Mosaiced target or background images
_asc	Post-calibration association table
_trl	Trailer file
_pdq	Processing Data Quality file

15.1.2 Science Data Files

The *_raw.fits, *_cal.fits, *_ima.fits, and *_mos.fits files are all defined as *science data files*, as they contain the images of interest for scientific analysis.

File Contents and Organization

The data for an individual NICMOS science image consist of five arrays, each stored as a separate image extension in the FITS file. The five data arrays represent:

- The science (SCI) image from the detector.
- An error (ERR) array containing statistical uncertainties (in units of 1 σ) of the science data.
- An array of bit-encoded data quality (DQ) flags representing known status or problem conditions of the science data.

- An array containing the number of data samples (SAMP) that were used to compute each science image pixel value.
- An array containing the effective integration time (TIME) for each science image pixel.

A grouping of the five data arrays for one science image is known as an *image set* or *imset*.

A science data file can contain one or more imsets. For example, an individual NICMOS exposure obtained with the ACCUM mode will generate a `*_raw.fits` file with one imset; an individual MULTIACCUM exposure with *x* readouts will generate a `*_raw.fits` file (and, after calibration, a `*_ima.fits` file) containing *x* + 1 imsets, including the zeroth readout. The files `*_cal.fits` and `*_mos.fits` files always contain one imset.

In a MULTIACCUM exposure, the order of the imsets in the file is such that the result of the longest integration time (the last readout performed on-board) occurs ***first*** in the file (first imset), the one readout before the last is the seond imset, and so on; the zeroth readout is the last imset (i.e., the order is in the opposite sense from which they are obtained).

Although the five science, error, data quality, samples, and integration time arrays associated with each imset are stored in a single file, they are kept separate as five individual FITS image *extensions* within the file. The order of the images in the FITS files is listed in Table 15.2 and shown graphically in Figure 15.1 and Figure 15.2. The examples given in Table 15.2 and Figure 15.2 refer to a MULTIACCUM image (multiple imsets), while Figure 15.1 refers to ACCUM, BRIGHTOBJ and RAMP images (one imset, namely extensions 1 through 5). Each extension comes with its own header, and each FITS file contains, in addition, a *primary header* (primary header-data unit or HDU).

The only contents of the primary HDU are header keywords. There is no image data in the primary header. The keywords in the primary header are termed *global keywords* because they apply to the data in all of the file extensions. The organization and location of header keywords is explained in detail later in the chapter.

Table 15.2: NICMOS Science Data File Contents

Header-Data Unit	Extension Name	imset	Contents	Datatype
Primary (Extension 0)	(N/A)	(N/A)	Global keywords; no data.	(N/A)
Extension 1	SCI	1	Science image	raw: 16-bit int; calibrated: float
Extension 2	ERR	1	Error (sigma) image	float
Extension 3	DQ	1	Data Quality image	16-bit int
Extension 4	SAMP	1	Number of Samples image	16-bit int
Extension 5	TIME	1	Integration Time image	float
Extension 6	SCI	2	Science image	raw: 16-bit int; calibrated: float
Extension 7	ERR	2	Error (sigma) image	float
Extension 8	DQ	2	Data Quality image	16-bit int
Extension 9	SAMP	2	Number of Samples image	16-bit int
Extension 10	TIME	2	Integration Time image	float
.....	.....	...	....	.....

Figure 15.1: Data Format for ACCUM, RAMP, BRIGHTOBJ and ACQ Modes

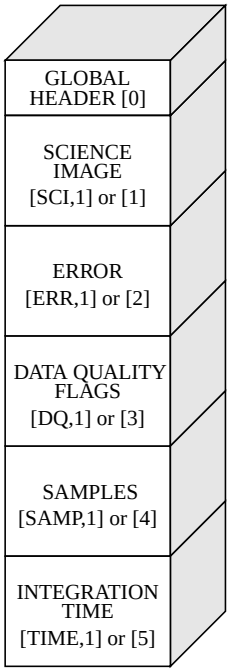

Figure 15.2: MULTIACCUM Mode Data Format

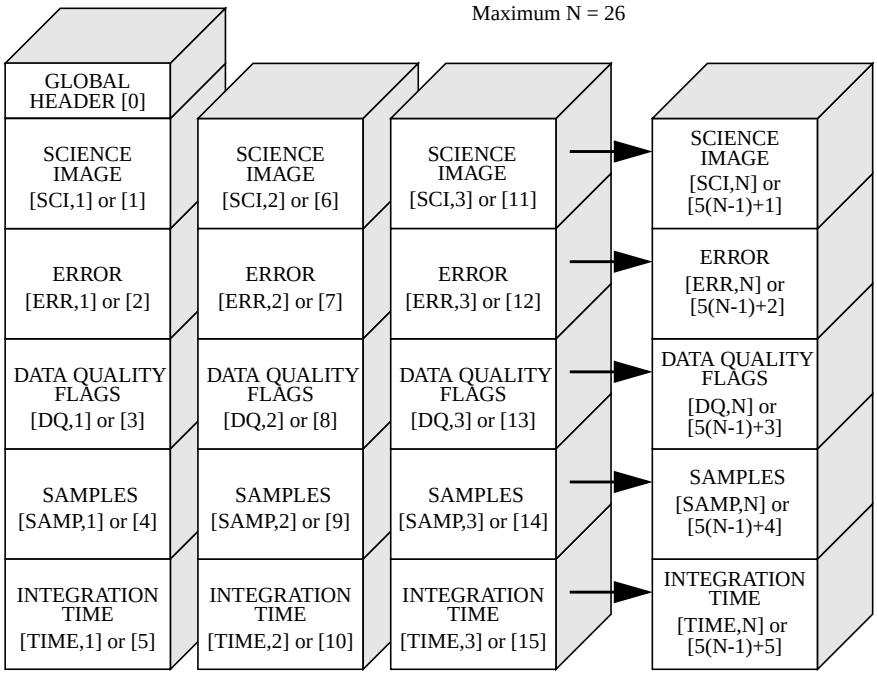

The following sections explain the contents and origin of each of the five image arrays in each imset in more detail.

Science Image

This image contains the data from the detector readout. In ACCUM, RAMP, and BRIGHTOBJ modes the image received from the instrument is the result of subtracting the initial from the final readouts of the exposure. In MULTIACCUM mode the images received are the raw (unsubtracted) data corresponding to each detector readout. In this case the subtraction of the zeroth read is done in the ground calibration pipeline task **calnica** (see Chapter 16). In raw datasets the science array is an integer (16-bit) image in units of DNs (counts). In calibrated datasets it is a floating-point image in units of DNs per second (count rates).

Error Image

The error image is a floating-point array containing the statistical uncertainty associated with each corresponding science image pixel. For all observing modes except RAMP, this image is computed in the ground calibration pipeline task **calnica** as a combination of detector read noise and Poisson noise in the accumulated science image counts (see Chapter 16) and is expressed in terms of 1σ uncertainties. In RAMP mode the instrument computes the variance for each pixel value from the intermediate readouts and returns the variance image to the ground where it is stored in the raw science data file (`*_raw.fits`). In this case the ground calibration pipeline simply converts the variance values in the raw data file to standard deviations.

Data Quality Image

This integer (unsigned 16-bit) array contains bit-encoded data quality flags indicating various status and problem conditions associated with corresponding pixels in the science image. Because the flag values are bit-encoded, a total of 16 simultaneous conditions can be associated with each pixel. Table 15.3 lists the flag values and their meanings.

Number of Samples Image

The SAMP image is an integer (16-bit) array containing the total number of data samples that were used to compute the corresponding pixel values in the science image. For RAMP mode observations this information is computed by the instrument and sent to the ground to be recorded in the raw data file (`*_raw.fits`). For ACCUM and BRIGHTOBJ modes, the number of samples contributing to each pixel is set to a value of 1 in the raw data file. For MULTIACCUM mode the sample values in the raw and intermediate data files are set to the number of readouts that contributed to the corresponding science image. Because the number of samples in the raw images for MULTIACCUM, ACCUM and BRIGHTOBJ modes have one number for all pixels of an imset, the array is usually not created (to save on data volume), and the value of the sample is stored in the header keyword PIXVALUE in the SAMP image extension (see Table 15.6 below).

In MULTIACCUM calibrated data files (`*_cal.fits`) the SAMP array contains the total number of valid samples used to compute the final science image pixel value, by combining the data from all the readouts and rejecting

Table 15.3: NICMOS Data Flag Values

Flag Value	Bit Setting[a]	Flag Meaning
0	0000 0000 0000 0000	No known problems
1	0000 0000 0000 000**1**	Reed-Solomon decoding error in telemetry
2	0000 0000 0000 00**1**0	Poor or uncertain Linearity correction
4	0000 0000 0000 0**1**00	Poor or uncertain Dark correction
8	0000 0000 0000 **1**000	Poor or uncertain Flat Field correction
16	0000 0000 000**1** 0000	Poor Background subtraction
32	0000 0000 00**1**0 0000	Defective (hot or cold) pixel
64	0000 0000 0**1**00 0000	Saturated pixel
128	0000 0000 **1**000 0000	Missing data in telemetry
256	0000 000**1** 0000 0000	Bad pixel determined by calibration
512	0000 00**1**0 0000 0000	Pixel contains Cosmic Ray
1024	0000 0**1**00 0000 0000	Pixel contains source
2048	0000 **1**000 0000 0000	(unassigned)
4096	000**1** 0000 0000 0000	User flag
8192	00**1**0 0000 0000 0000	User flag
16384	0**1**00 0000 0000 0000	Reserved

a. Most significant bit is at left.

cosmic ray hits and saturated pixels. In this case the sample array may have different values at different pixel locations (less or equal to the total number of samples in the MULTIACCUM sequence), depending on how many valid samples there are at each location.

In the mosaic images (`*_mos.fits`), the data in the SAMP array indicate the number of samples that were used from overlapping images to compute the final science image pixel value.

Integration Time Image

The TIME image is a floating-point array containing the effective integration time associated with each corresponding science image pixel value. These data are always computed in the ground calibration pipeline for recording in the raw data file. For ACCUM and BRIGHTOBJ mode observations each pixel has the same time value. For MULTIACCUM observations each pixel for a given readout has the same time value in the raw and intermediate data. Therefore, the same data-volume-saving technique is used in these cases: the array is not created and the value of the time is stored in the header keyword PIXVALUE in the TIME image extension (see Table 15.6 below). For RAMP mode observations the integration time for each pixel is computed from the exposure time per sample and

the total number of samples contributing to each pixel; a TIME array is thus returned to the ground.

In MULTIACCUM calibrated data files (`*_cal.fits`) the TIME array contains the combined exposure time of all the readouts that were used to compute the final science image pixel value, after rejection of cosmic ray and saturated pixels from the intermediate data. As in the case of the SAMP array, the TIME array can have different values at different pixel locations, depending on how many valid samples compose the final science image in each pixel.

In mosaic images (`*_mos.fits`), the TIME array values indicate the total effective exposure time for all the data that were used to compute the final science image pixel values.

15.1.3 Auxiliary Data Files

The `*_spt.fits`, `*_trl.fits`, `*_pdq.fits`, the `*_asn.fits`, and the `*_asc.fits` files are termed *auxiliary data files*. They contain supporting information on the observation, such as spacecraft telemetry and engineering data, assessment of the quality of the observation, calibration information, and information on the associations present in the observations.

Association Tables

The *association tables*, `*_asn.fits` and `*_asc.fits`, are FITS binary tables which are created when a particular observation generates an association of datasets (see “Associations” on page B-4). In particular, the `*_asn.fits` table is generated by OPUS, and contains the list of datasets which make up the association (e.g., from a dither or chop pattern). The `*_asn.fits` tables are the inputs to the pipeline **calnicb**, which creates the mosaiced or background subtracted images (`*_mos.fits` files) from the input datasets. All the datasets must have been processed through the basic pipeline data reduction (**calnica**) before being processed through **calnicb**. In addition to the output science image(s), **calnicb** produces another associations table (`*_asc.fits`), which has the same content as the `*_asn.fits` table, along with additional information on the offsets used by the pipeline for reconstructing the science image. For mosaics (dither patterns), there is only one final image produced, with file name `*0_mos.fits`. For chop patterns, in addition to the background-subtracted image of the target (`*0_mos.fits`), an image for each background position will be produced; the file names of these background images are `*1_mos.fits`, `*2_mos.fits`,..., `*8_mos.fits` (A maximum of eight independent background positions is obtainable with the NICMOS patterns, see the *NICMOS Instrument Handbook* for details).

Support File

The support files `*_spt.fits` contain information about the observation and engineering data from the instrument that was recorded at the time of the observation. A support file can have multiple extensions within the same file; in the case of a MULTIACCUM observation there will be one extension for each

readout (i.e., each imset) in the science data file. Each extension in the support file holds an integer (16-bit) image.

Trailer File

The trailer files `*_trl.fits` contain information on the calibration steps executed by the pipelines and diagnostics issued during the calibration.

Processing Data Quality File

The processing data quality files (`*_pdq.fits`) contain general information summarizing the observation, a data quality assessment section, and a summary on the pointing and guide star lock. They state whether problems were encountered during the observations, and, in case they were, describe the nature of the problem. There is one `*_pdq.fits` file produced for each dataset, and, in case of associations, one `*_pdq` file for each NICMOS product (i.e., each `*_mos.fits` file).

15.2 Header Keywords

Both the primary header and the headers of each image extension in a science data file contain *keywords*. The keywords store a wide range of information about the observations themselves (e.g., observing mode, integration time, filters or grisms), the processing of the data by the OPUS pipeline (e.g., calibration steps performed and reference files used), and the properties of the data themselves (e.g., number of image extensions, dimensions and data type of each image, coordinate system information, flux units, and image statistics).

The primary header carries global keywords which are applicable to all extensions; the modification of a keyword in the primary header has the effect of changing the value seen by all extensions. In addition to the common keywords, the extension headers carry extension-specific keywords, which contain information relevant to the image in a particular extension. For example, observation parameters, calibration switches and reference file names are contained in the primary header. Exposure time and coordinate information, on the other hand, is contained in the header of each image extension because this information could vary from one group of extensions to another.

Table 15.4 below lists most of the keywords in the primary header of the *science data files*; the observer may find many of them useful. A complete description of the keywords can be found at the following WWW page:

`http://archive.stsci.edu/keyword`

Table 15.5 lists some of the relevant keywords that are specific to image extensions; they appear in the extension headers, but not in the primary header:

In the SCI image extensions, additional keywords describing the data quality are present. They give the number of pixels which have a flag different from zero in the DQ extension, and a suite of statistical information (mean, standard

Table 15.4: Science Data File Primary Header Keywords

Keyword Name	Meaning
	Image Keywords
NEXTEND	Number of extensions in the file (up to 130 for MULTIACCUM).
FILENAME	Name of the file
FITSDATE	Date on which the FITS file was generated
FILETYPE	Type of data: SCI - Science Data File SPT - Support File ASN_TABLE - Association Table
TELESCOP	HST
INSTRUME	Instrument used (NICMOS)
EQUINOX	Equinox of the celestial coordinate system (J2000.0 for HST observations)
	Data Description Keywords
ROOTNAME	Rootname (IPPPSSOOT) of the dataset
IMAGETYP	Image type EXT = external image FLAT = flatfield image DARK = dark image
PARALLEL	Indicates if the observation was taken in parallel
PRIMESI	Primary Instrument used for the observation
	Target Information
TARGNAME	Proposer's target name
RA_TARG	Right Ascension of the target (degrees, J2000)
DEC_TARG	Declination of the target (degrees, J2000)
	Proposal Information
PROPOSID	Proposal's identification number
LINENUM	Exposure's logsheet linenumber, from the Phase 2 proposal
	Exposure Information
ORIENTAT	Position angle of the image y axis (degrees East of North)
FGSLOCK	Commanded FGS lock (FINE, COARSE, GYROS, UNKNOWN)
DATE-OBS	UT date of start of the observation (dd/mm/yy)
TIME-OBS	UT time of start of the observation (hh:mm:ss)
EXPSTART	Exposure start time (Modified Julian Date)
EXPEND	Exposure end time (Modified Julian Date)
EXPTIME	Total integration time (sec)

Table 15.4: Science Data File Primary Header Keywords (Continued)

Keyword Name	Meaning
	Instrument Configuration Information
CAMERA	NICMOS camera used in the observation (1, 2, or 3)
PRIMECAM	NICMOS Prime Camera during the observation (for internal parallels)
FOCUS	In-focus camera for this observation
APERTURE	Aperture used in the observation (NICi, NICi-FIX, NIC2-CORON)
OBSMODE	Observing mode (MULTIACCUM, ACCUM,...)
FILTER	Filter or grism used
NUMITER	Number of iterations in the exposure
NREAD	Number of ACCUM initial and final readouts
NSAMP	Number of MULTIACCUM or RAMP samples
SAMP_SEQ	MULTIACCUM exposure time sequence name
PATT_OFF	Pattern offset method (SAM, SAM-NO-REACQ, etc.)
PATTERN	Pattern type
PFRAME	Reference frame of pattern (DETECTOR, SKY)
PORIENT	Pattern orientation on the sky relative to North-to-East (degrees)
NUMPOS	Number of positions in the pattern
DITHSIZE	Size of the dither steps (arcseconds)
CHOPSIZE	Size of the chop steps (arcseconds)
PATT_POS	Position number of the exposure in the pattern sequence
FOMXPOS	X offset of the Camera FOV using NICMOS FOM (arcsec)
FOMYPOS	Y offset of the Camera FOV using NICMOS FOM (arcsec)
NFXTILTP	FOM X-tilt position (arcsec)
NFYTILTP	FOM Y-tilt position (arcsec)
NPXTILTP	PAM X-tilt position (arcsec)
NPYTILTP	PAM Y-tilt position (arcsec)
NPFOCUSP	PAM focus position (deg)
READOUT	Detector array readout rate (FAST, SLOW)
SAMPZERO	Sample time of MULTIACCUM zeroth read (sec)
ADCGAIN	Analog-digital conversion gain (electrons/DN)
	Photometry Keywords
PHOTMODE	Combination of <INSTRUME>+<CAMERA>+<FILTER>

Table 15.4: Science Data File Primary Header Keywords (Continued)

Keyword Name	Meaning
PHOTFLAM	Inverse sensitivity (erg/cm^2/angstrom/DN)
PHOTFNU	Inverse sensitivity (Jy*sec/DN)
PHOTZPT	ST magnitude system zero point
PHOTPLAM	Pivot wavelength of the photmode (Angstrom)
PHOTBW	Root Mean Square bandwidth of the photmode (Angstrom)
	Calnica Calibration Reference Files (inputs to calnica)
MASKFILE	Static data quality file
NOISFILE	Detector read noise file
NLINFILE	Detector non-linearity file
DARKFILE	Dark current file
FLATFILE	Flat field file
PHOTTAB	Photometric calibration table
BACKTAB	Background model parameters table
	Calnica Calibration Reference File Pedigree (outputs from calnica)
MASKPDGR	Static data quality file pedigree (values: GROUND dd/mm/yyyy - for reference files originated from Thermal Vacuum data; INFLIGHT dd/mm/yyyy - for reference files originated from on-orbit calibration observations)
NOISPDGR	Detector read noise file pedigree (values: GROUND dd/mm/yyyy; INFLIGHT dd/mm/yyyy)
NLINPDGR	Detector non-linearity file pedigree (values: GROUND dd/mm/yyyy; INFLIGHT dd/mm/yyyy)
DARKPDGR	Dark current file pedigree (values: GROUND dd/mm/yyyy; INFLIGHT dd/mm/yyyy; and MODEL dd/mm/yyyy for the synthetic darks, see next Chapter)
FLATPDGR	Flat field file pedigree (values: GROUND dd/mm/yyyy; INFLIGHT dd/mm/yyyy)
PHOTPDGR	Photometric calibration table pedigree (values: GROUND dd/mm/yyyy; INFLIGHT dd/mm/yyyy)
BACKPDGR	Background model parameters table pedigree (values: GROUND dd/mm/yyyy; INFLIGHT dd/mm/yyyy)
	Calnica Calibration Switches (allowed values: PERFORM, OMIT)
BIASCORR	Correct wrapped pixel values
ZSIGCORR	MULTIACCUM zero read signal correction
ZOFFCORR	Subtract MULTIACCUM zero read
MASKCORR	Data quality initialization (DQ array)
NOISCALC	Calculate statistical errors (ERR array)

Table 15.4: Science Data File Primary Header Keywords (Continued)

Keyword Name	Meaning
NLINCORR	Correct for detectors non-linearities
DARKCORR	Dark correction
FLATCORR	Flat-field correction
UNITCORR	Convert to count rate
PHOTCALC	Populate photometry keywords
CRIDCALC	Identify cosmic ray hits (update of DQ arrays in *_ima.fits output of calnica for MULTIACCUM)
BACKCALC	Calculate background estimates
WARNCALC	Generate user warnings
Calnica Calibration Indicators (output from calnica; values: PERFORMED, SKIPPED, OMITTED)	
BIASDONE	Correct wrapped pixel values
ZSIGDONE	MULTIACCUM zero read signal correction
ZOFFDONE	Subtract MULTIACCUM zero read
MASKDONE	Data quality initialization (DQ array)
NOISDONE	Calculate statistical errors (ERR array)
NLINDONE	Correct for detectors non-linearities
DARKDONE	Dark correction
FLATDONE	Flat-field correction
UNITDONE	Convert to count rate
PHOTDONE	Populate photometry keywords
CRIDDONE	Identify cosmic ray hits (update of DQ arrays in *_ima.fits output of calnica for MULTIACCUM)

Table 15.4: Science Data File Primary Header Keywords (Continued)

Keyword Name	Meaning
BACKDONE	Calculate background estimates
WARNDONE	Generate user warnings
	Calibration Status
CALSTAGE	State of the calibration (values: CALNICA, CALNICB, UNCALIBRATED)
CAL_VER	Version number of the CALNIC code
	Calnicb Calibration Information
ILLMCORR	Subtraction of background illumination pattern reference image (input values: PERFORM, OMIT)
ILLMDONE	Subtraction of background illumination pattern reference image (output values: PERFOMED, SKIPPED, OMITTED)
ILLMFILE	Background illumination pattern reference image filename
ILLMPDGR	Background illumination pattern file pedigree
MEAN_BKG	Mean background level (DN/sec), computed by calnicb
	Association Keywords
ASN_ID	Association rootname
ASN_TAB	Name of the association table
ASN_MTYP	Role of the dataset in the association (e.g., targe, ; first background, second background, etc.; allowed values: EXP_TARG, EXP_BCKn, PROD_TARG, PROD_BCKn, where EXP=input exposure, PROD=output image, TARG=target, BCK=background, n=1-8)

deviation, minimum and maximum of good pixels in the entire detector and per quadrant) on the image.

Keywords giving the data on the ephemeris and engineering data on the status of the telescope and of the instrument during the observations are reported in the support file, `*_spt.fits`. Table 15.6 describes some of the relevant keywords from this file.

15.3 Working with NICMOS Files

The quickest way to learn how each observation was performed is to use the **iminfo** task in the STSDAS **toolbox.headers** package to look at the headers of the science data. The output from **iminfo** summarizes on one screen the relevant information about an observation (Table 15.7) and the instrument configuration

Table 15.5: Image Extension Header Keywords in Science Data Files

Keyword Name	Meaning
	Data Description Keywords
EXTNAME	Name of the extension in an imset of the data file (SCI, ERR, DQ, SAMP, TIME)
EXTVER	Extension version; integer number to uniquely identify an IMSET in a science data file. A MULTIACCUM file can contain up to 26 IMSETs, i.e. up to EXTVER=26.
INHERIT	Switch to allow the image extension header to inherit the primary header keywords. Allowed values: T=TRUE, F=FALSE.
DATAMIN	Minimum pixel value
DATAMAX	Maximum pixel value
BUNIT	Brightness units; allowed values: COUNTS, COUNTS/S.
PIXVALUE	When ALL pixels in an image extension have the same value (e.g., the SAMP and TIME arrays in the *_ima.fits file from a MULTIACCUM exposure or the ERR, DQ, SAMP and TIME arrays in the *_raw.fits files from a MULTIACCUM, ACCUM or BRIGHTOBJ exposure) the pixel array of that extension is not generated, and the PIXVALUE keyword is instead populated with the common value of the pixels.
	World Coordinate System of Image
CRPIX1	x-coordinate of image's reference pixel
CRPIX2	y-coordinate of image's reference pixel
CRVAL1	RA of reference pixel (degrees)
CRVAL2	DEC of reference pixel (degrees)
CD1_1	Partial derivative of RA with respect to x
CD1_2	Partial derivative of RA with respect to y
CD2_1	Partial derivative of Dec with respect to x
CD2_2	Partial derivative of Dec with respect to y
	Readout Parameters
SAMPNUM	Sample number of the MULTIACCUM sequence
SAMPTIME	Total integration time (sec)
DELTATIM	Integration time of the sample (sec)
ROUTTIME	UT time of array readout (MJD)

Table 15.6: NICMOS Primary Header Keywords in the Support Files

Keyword Name	Meaning
PA_V3	Position angle of the V3 axis of HST (degrees)
RA_V1	RA of the V1 axis of HST (degrees in J2000)
DEC_V1	DEC of the V1 axis of HST (degrees in J2000)
RA_SUN	RA of the Sun (degrees in J2000)
DEC_SUN	DEC of the Sun (degrees in J2000)
RA_MOON	RA of the Moon (degrees in J2000)
DEC_MOON	DEC of the Moon (degrees in J2000)

during the observations (Table 15.8), by reading and reporting the value of the appropriate keywords.

Table 15.7: Observation Information in iminfo Listing

Field Descriptor	Header Keyword Source
Rootname	ROOTNAME
Instrument	INSTRUME
Target Name	TARGNAME
Program	ROOTNAME (positions 2–4)
Observation set	ROOTNAME (positions 5–6)
Observation	ROOTNAME (positions 7–8)
File Type	FILETYPE
Obs Date	DATE-OBS or FPKTTIME
Proposal ID	PROPOSID
Exposure ID	PEP_EXPO
Right Ascension	CRVAL1
Declination	CRVAL2
Equinox	EQUINOX

The entire suite of keywords from any header can be listed with the IRAF task **imheader**. Given that NICMOS data files contain multiple extensions, the number of the desired extension must always be specified. For example, to list the primary header content of a calibrated image, you type

```
cl> imheader n0g70106t_cal.fits[0] long+ | page
```

where [0] identifies the primary header. To list the header of the *second* science image in a MULTIACCUM sequence (the sixth extension):

Table 15.8: NICMOS-Specific Information in iminfo Listing

Field Descriptor	Header Keyword Source
Image type	IMAGETYP
Number of extensions	NEXTEND
Camera number	CAMERA
Aperture	APERTURE
Filter name	FILTER
Observation Mode	OBSMODE
Number of initial/final reads	NREAD (ACCUM)
Number of intermediate samples	NSAMP (MULTIACCUM or RAMP)
MULTIACCUM sequence	SAMP_SEQ
Exposure time (sec)	EXPTIME
Readout speed	READOUT
Association ID	ASN_ID
Number of Iterations	NUMITER
Calibration steps done	Switches whose values are set to “PERFORMED”. Switches are: ZOFFDONE, MASKDONE, BIASDONE, NOISDONE, DARKDONE, NLINDONE, FLATDONE, UNITDONE, PHOTDONE, CRIDDONE, BACKDONE, WARNDONE

```
cl> imheader n0g70106t_cal.fits[6] long+ | page
```

An example of a header listing is shown in Figure 15.3 below.

Figure 15.3: Long imheader

Chapter 2 describes in detail how to work with FITS file extensions. Here we will recap the essentials. In order to simplify access to NICMOS FITS image extensions, each extension header contains the two keywords: EXTNAME (extension name) and EXTVER (extension version number). The EXTNAME keyword identifies the nature of the extension (SCI, ERR, DQ, SAMP, TIME, see Table 15.7). The EXTVER keyword contains an integer value which is used to uniquely identify a particular imset (quintuple of image extensions). For example, the five image extensions (single imset) contained in the science data file for an ACCUM, RAMP, or BRIGHT OBJECT observation will all usually be assigned an EXTVER value of 1 because there will only be one group of extensions in the file. In a MULTIACCUM science data file, each group of extensions associated with a given readout will have a unique EXTVER value, running from 1 up to the total number of readouts in that particular file.

To list the header of the *second* science image in a MULTIACCUM sequence, in addition to the command line above, one can give:

```
cl> imheader n0g70106t_cal.fits[sci,2] long+ | page
```

In general, to access a particular image extension, append the name and version number of the desired extension in square brackets to the end of the file name. The EXTNAME value is specified first, then the EXTVER value, separated by a comma. Indeed, the use of the keywords EXTNAME and EXTVER is not limited to the task **imheader,** but can be used in all IRAF tasks.

The primary header data unit in a NICMOS FITS file does not contain the EXTNAME or EXTVER keywords. The absolute extension number 0 (zero) refers to the primary header.

If a calibration keyword needs to be changed, the IRAF/STSDAS **chcalpar** task can be used. For instance, to modify the flatfield calibration from PERFORM to OMIT in a given data file, the following command can be given:

```
cl> chcalpar n0g70106t_raw.fits
```

The pset list appropriate for the image will appear, and the calibration keyword can be modified. The operation performed with **chcalpar** can be equivalently performed (although in a more cumbersome way) with the general IRAF task **hedit**; in this case, the extension [0] of the primary header must be explicitly specified:

```
cl> hedit n0g70106t_raw.fits[0] flatcorr OMIT
```

Do not try to edit a keyword in an extension header unless you are certain that the keyword does not reside in the primary header. (See “Header Keywords and Inheritance” on page 2-6).

Image sections can be specified in the case of NICMOS data with the same syntax as all IRAF images. For example, to specify a pixel range from 101 to 200 in the *x* direction and all pixels (denoted by an asterisk) in the *y* direction from the second error image in a file, the complete file name specification would be `n0g70106t_cal.fits[err,2][101:200,*]`.

If you use both extension and image section syntax together, the extension name or number must come first enclosed in one set of brackets, and the image section specification in a second set of brackets.

15.4 From the Phase II Proposal to Your Data

The connection between the Exposure Logsheet that each observer fills out during the Phase II proposal process and the datasets and associations that the observer receives once the observations are executed can be better understood through some examples.

The first example shows an exposure logsheet entry that will generate only one dataset:

```
Exposure_Number: 1
Target_Name: HDF
Config: NIC2
Opmode: MULTIACCUM
Aperture: NIC2
Sp_Element: F160W
Optional_Parameters: SAMP-SEQ=STEP256,NSAMP=12
NUMBER_of_Iterations: 1
Time_Per_Exposure: DEF
Special_Requirements: POS TARG 0.5, 0.5
```

The science data file in the dataset will contain 13 imsets (corresponding to the MULTIACCUM NSAMP=12 parameter), and some of the header keywords will be filled with the relevant information from the target and exposure logsheets of the Phase II (e.g., the keywords TARGNAME, RA_TARG, DEC_TARG,....).

The next example shows an exposure logsheet entry that will generate both multiple datasets and an association:

```
Exposure_Number: 1
Target_Name: HDF
Config: NIC2
Opmode: MULTIACCUM
Aperture: NIC2
Sp_Element: F160W
Optional_Parameters:PATTERN=SPIRAL-DITH-CHOP,NUM-POS=8,
DITH-SIZE=1.5,CHOP-SIZE=0.75,SAMP-SEQ=STEP256,NSAMP=12
Number_of_Iterations: 1
Time_Per_Exposure: DEF
Special_Requirements:
```

In this observation, eight datasets (one for each position of the pattern) and one association will be created. The pipeline products will include the eight reduced datasets, one mosaic of the background-subtracted target, and one mosaic of the background.

An association will be generated also in the case below:

```
Exposure_Number: 1
Target_Name: HDF
Config: NIC2
Opmode: MULTIACCUM
Aperture: NIC2
Sp_Element: F160W
Optional_Parameters: SAMP-SEQ=STEP256,NSAMP=12
NUMBER_of_Iterations: 3
```

```
Time_Per_Exposure: DEF
Special_Requirements:
```

The number of iterations is 3, implying that three datasets will be generated from this exposure logsheet, plus an association table containing the three datasets. The collection of multiple iterations into an association is a new feature introduced by the NICMOS and STIS pipelines. In our specific example, The co-added image from the three iterations will be one of the products of the pipeline.

15.5 Paper Products

After the data from an observation have been received and processed through the STScI pipeline, hardcopy products (*paper products*) are generated which summarize the data obtained. The paper products are sent to the observer together with the data to provide a first look at the observations and their quality. Here we briefly describe the NICMOS paper products.

Paper products typically summarize the set of exposures that constitute a visit in the Phase II proposal. The set of exposures can be either individual datasets or associations. Paper products are produced by accessing the appropriate keywords in the dataset headers or in the association tables.

A given page of the NICMOS paper products falls into one of two categories: visit-level page or exposure-level page. The content of the pages is as follows:

Visit-Level Pages

- ***Cover Page***: contains the proposal ID, the visit number, the PI's last name, and the proposal title.
- ***Explanatory Notes***: a set of notes explaining the information contained in the paper products.
- ***Target List***: a table listing the targets of the observations being summarized (Figure 15.4).
- ***Observation Summary***: a table summarizing the proposal information for each exposure in the present set, including processing and data quality flags (Figure 15.4).
- ***Optional Parameters***: a table listing the optional parameters, other than the Pattern related parameters, used in the observations (Figure 15.4).
- ***Observing Pattern Strategy***: a table listing the observing pattern used for each exposure in the set (Figure 15.5).

Exposure-level Pages

- ***Exposure Plots***: a graphical representation of the data contained in each exposure, including the final calibrated science image and, in case of associations, successive pages containing a cartoon of the observing pattern plus the on-target and background individual images (Figure 15.6, Figure 15.7, and Figure 15.8).
- ***Data Quality Summary***: a summary of the spacecraft performance, pipeline processing status, and calibration data quality for each exposure.
- ***Calibration Reference File Summary***: a summary of the calibration processing switches and reference files used to process each exposure (Figure 15.9).

Figure 15.4: Target List, Observation Summary, and Optional Parameters

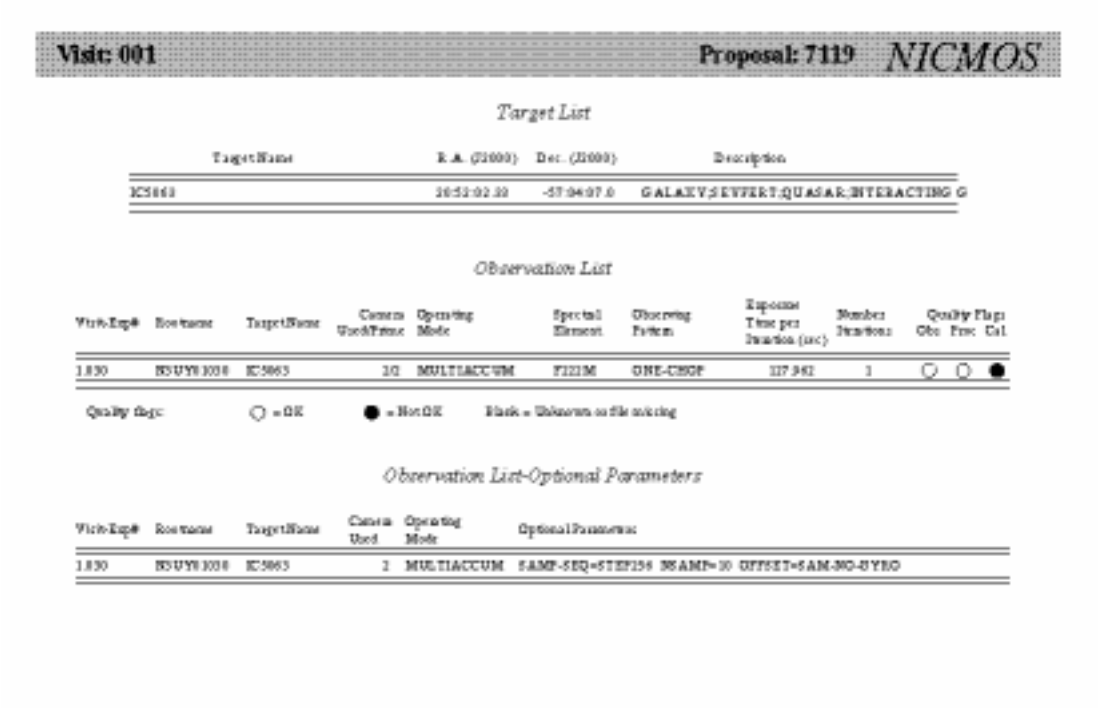

Figure 15.5: Observing Pattern Strategy

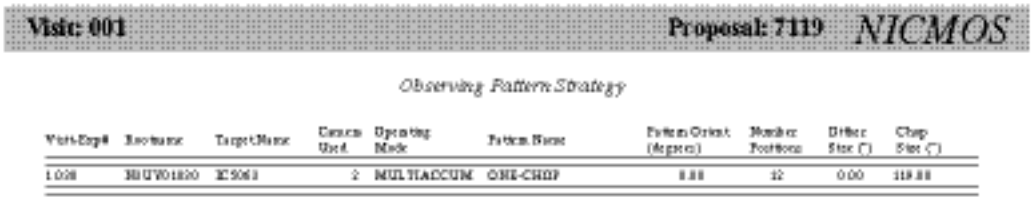

Figure 15.6: Individual Exposures

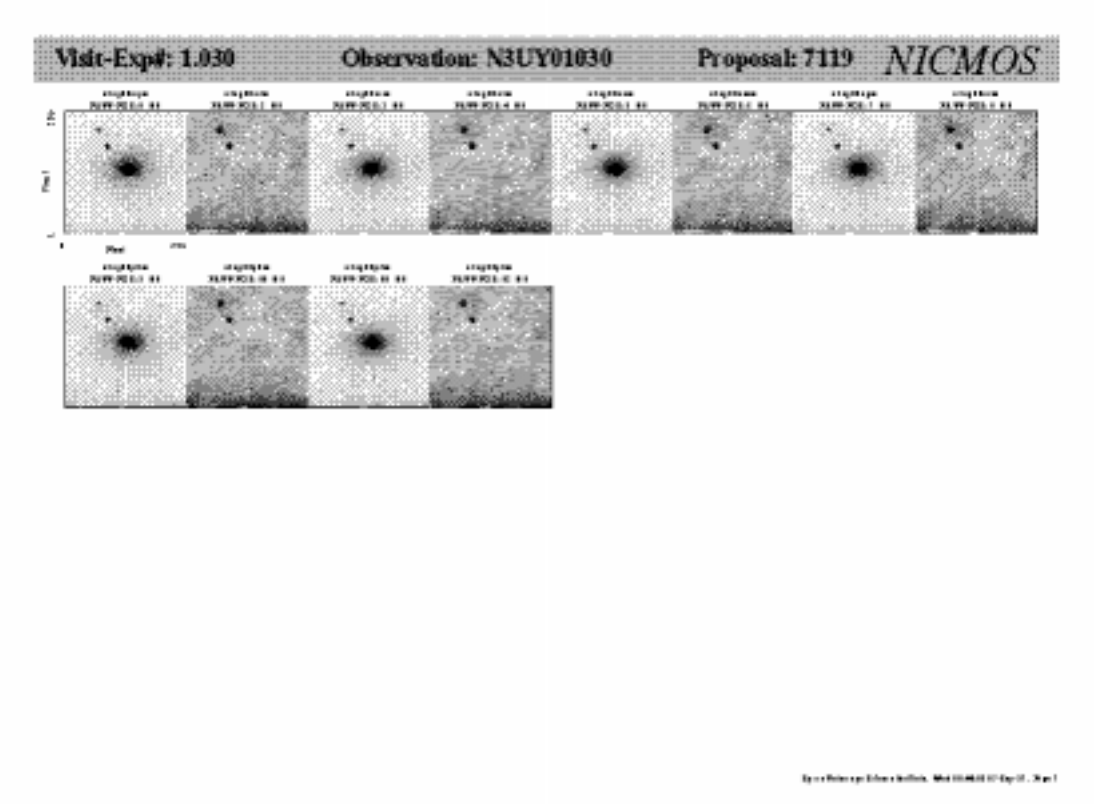

Figure 15.7: Calibrated Science Image

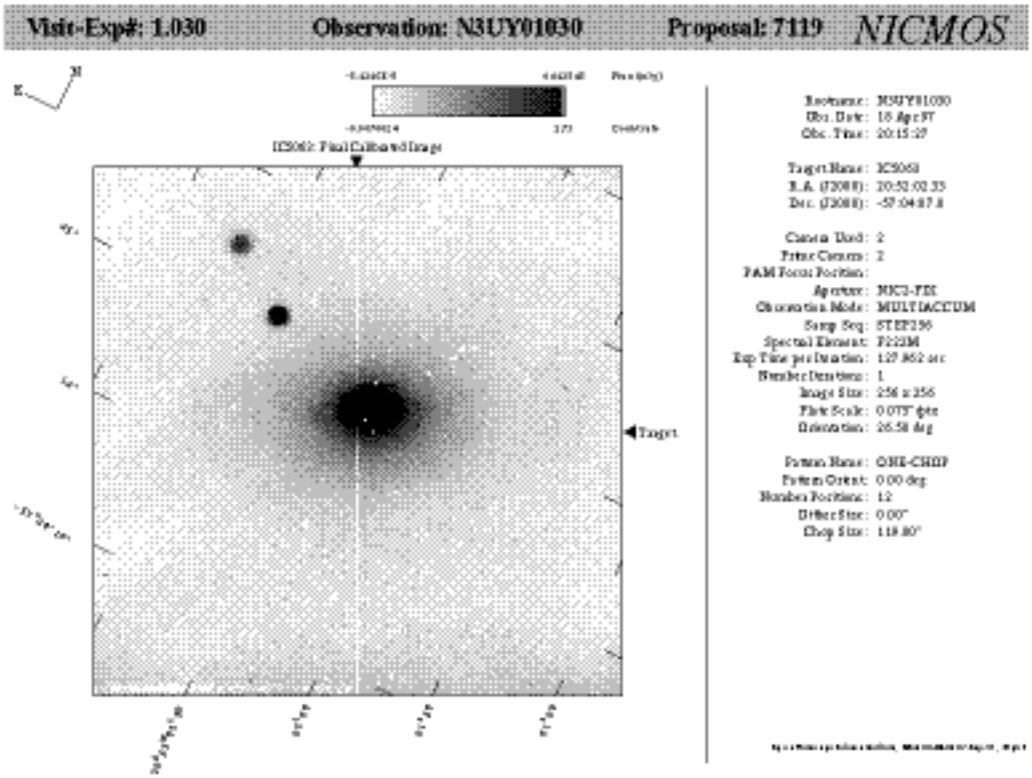

Figure 15.8: On-Target/Background Individual Images

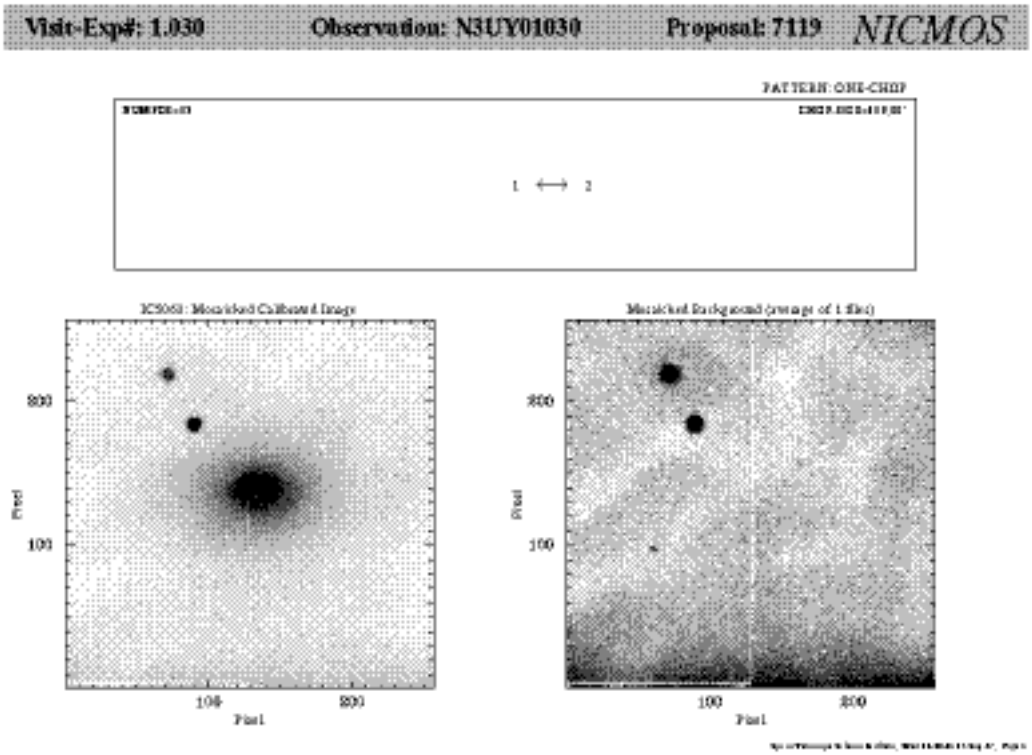

Figure 15.9: Calibration Status Summary

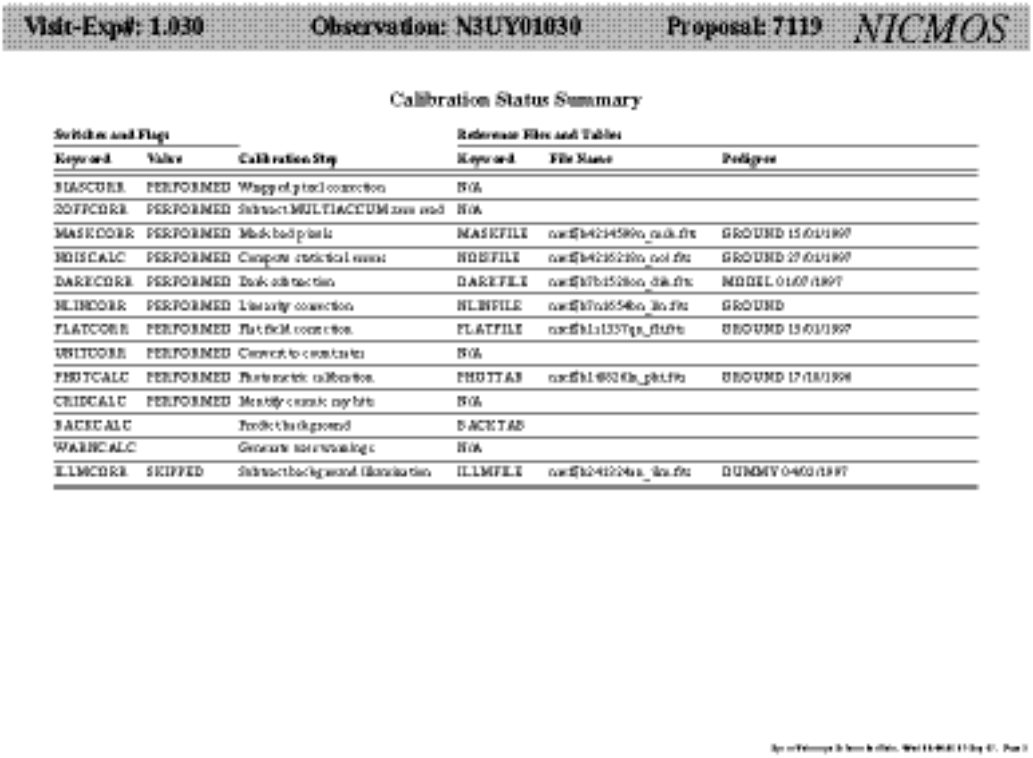

Chapter 16
NICMOS Calibration

In This Chapter...

This chapter is designed to help you understand what steps are performed on your data in the routine pipeline process and to help you decide whether you should recalibrate your data with different reference files. In this chapter we:

- Provide flowcharts and descriptions of the NICMOS pipeline calibration steps.
- Explain how to recalibrate your data using the calibration software in STSDAS.

16.1 Pipeline Processing

Shortly after your data arrive at STScI they pass through the OPUS *pipeline* which processes and calibrates them. All of the steps performed by the pipeline are recorded in the trailer file for your dataset (`*_trl.fits`). The main steps performed by the pipeline are:

1. The data are partitioned (separated into individual files, e.g., engineering and science data are separated).
2. The data are edited, if necessary, to insert fill in place of missing data.
3. The data are evaluated to determine discrepancies between the subset of the planned and executed observational parameters.

4. A list of calibration reference files to be used in the calibration of the data is created based on the executed observational parameters. This step does not generate comments in the NICMOS trailer file.
5. The data are converted to a generic (FITS) format and the header keyword values are populated (known as *generic conversion*).
6. The data are calibrated using a standard set of NICMOS calibration algorithms (**calnica** and **calnicb**).

The calibration software used by the pipeline (step 6 above) is exactly the same as that provided within STSDAS (see below). The calibration files and tables used are taken from the Calibration Data Base System (CDBS) at STScI and are the most up-to-date calibration files appropriate for the instrument configuration used in the observation.

16.2 NICMOS Calibration Software

16.2.1 The Calibration Pipeline

The science data that an observer receives are calibrated in the pipeline by at least one, and possibly two, STSDAS calibration routines: **calnica** and **calnicb**. The two routines perform different operations:

1. **calnica:** This routine removes the instrumental signature from the science data. It is the first calibration step, and is applied to *all* NICMOS datasets individually. **Calnica** operates on the raw science data files.
2. **calnicb**: This routine operates on *associations*: it co-adds datasets obtained from multiple iterations of the same exposure, mosaics images obtained from dither patterns, and background-subtracts images obtained from chop patterns. **Calnicb** is applied to the calibrated science data files (output from **calnica**), and requires association tables and the `*_spt.fits` files.

Both tasks determine which calibration steps are to be performed by looking at the values of the *calibration switches* keywords in the primary header of the input science data files (see Table 15.5). The tasks select the reference files to use in the calibration of the data by retrieving the reference file names from the *reference file* keywords. The appropriate values of the calibration switches and reference file keywords depend on the instrumental configuration used, the date when the observations were taken, and any special pre-specified constraints. They are set in the headers of the raw data file in the pipeline during the generic conversion process. The *calibration indicators* keywords record which steps have been performed on the data, and get updated after processing. In particular, the indicators for completed steps will have been assigned the value “PERFORMED”, while the indicators for the steps that were not performed will have been set to “OMITTED” or “SKIPPED”. The calibration indicators keywords should be examined in the primary header of the calibrated science data (`*_cal.fits`) to determine what calibration steps were applied to the data.

The **calnica** and **calnicb** tasks are available in STSDAS under the **hst_calib$nicmos** package. By using these tasks, observers can recalibrate data using the same software as the routine calibration pipeline at STScI.

16.2.2 Grism Spectroscopy

A unique capability of NICMOS is the grism mode, which permits multi-object, slitless spectroscopy at low resolution. Grism data are processed with separate calibration software, **calnicc**, which performs a series of steps that identify and extract spectra from the images. The inputs to **calnicc** are the calibrated images (`*_cal.fits`) produced by **calnica**.

Calnicc was developed using the Interactive Data Language (IDL) software at the Space Telescope European Coordinating Facility (ST-ECF). Currently **calnicc** *is not part of the automatic pipeline processing*, and users must apply the calibration software to their grism images. The manual (written by W. Freudling and R. Thomas) describing the software, its installation, and use can be found at the following WWW address:

`http://ecf.hq.eso.org/nicmos/calnicc/calnicc.html`

Most users will want to start the spectrum extraction processing using **NICMOSlook**, the interactive counterpart to **calnicc**. **NICMOSlook** is written in IDL, and is a quick-look spectrum extraction tool for grism spectra. Unlike **calnicc**, **NICMOSlook** requires users to specify parameters interactively (e.g., the best way to find an object, the weights to be given in the spectral extraction). This tool is recommended for first-time users or users with a small number of grism data. Once you are familiar with the extraction process and parameters, use **calnicc**. The user manual (written by W. Freudling, R. Thomas, and L. Yan), the software, and instructions for its installation can be found at the ST-ECF WWW address:

`http://ecf.hq.eso.org/nicmos/nicmoslook`

In this handbook, the main steps of the reduction and extraction performed by **calnicc** will be described.

You cannot run either **calnicc** or **NICMOSlook** unless you have an IDL licence.

16.3 Basic Data Reduction: calnica

The **calnica** task (Figure 16.1) operates on individual NICMOS datasets and performs the job of removing the instrumental signature from the raw science data. The **calnica** task also tries to identify cosmic ray hits in the MULTIACCUM images.

Figure 16.1: Conceptual calnica Pipeline; CDB is the Calibration DataBase

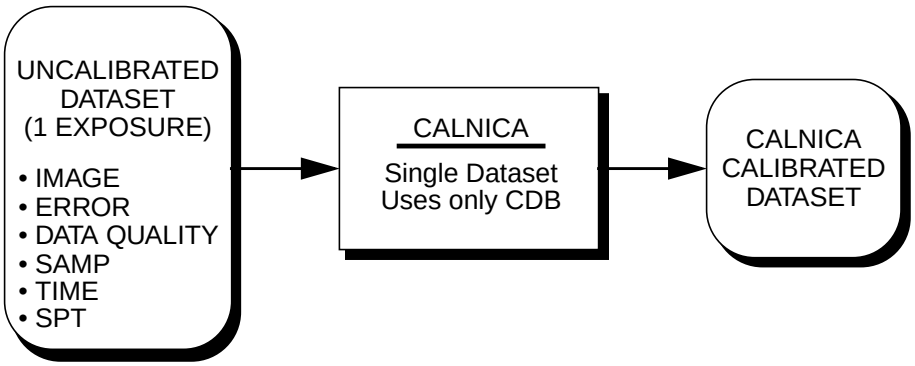

The inputs to **calnica** are the raw science (`*_raw.fits`) files. The output of **calnica** is usually a single file containing the *calibrated* science data (`*_cal.fits`). For MULTIACCUM mode datasets there is an additional intermediate output file (`*_ima.fits`) which contains the *calibrated* data from all the intermediate readouts. The `_ima.fits` data are fully calibrated up to, but not including, the cosmic ray rejection. The format and contents of the input and output science data files are identical so that the output data can be reused as input to **calnica**, if desired. One could, for example, process a science data file through some subset of the normal calibration steps performed by **calnica**, examine or modify the results, and then process the data through **calnica** again, performing other calibration steps or using alternate calibration reference files.

Figure 16.2 shows the portion of a calibrated NICMOS science file header containing the switches and reference file keywords that pertain to the processing performed by **calnica**. The accompanying flow chart (Figure 16.3) shows the sequence of **calnica** calibration steps, the input data and reference files and tables, and the output data file. Each calibration step is described in detail in the following sections.

ZOFFCORR

The ZOFFCORR step of **calnica** performs the subtraction of the zeroth read from all readouts in a MULTIACCUM file. This step is performed for data generated by the MULTIACCUM readout mode only. For other readout modes, the subtraction of the zeroth read is performed on-board, because the images returned to the ground are formed by taking the difference of initial and final non-destructive detector readouts.

The pipeline will subtract the zeroth read image from all readouts, including the zeroth read itself. Furthermore, the self-subtracted zeroth-read image will be propagated through the remaining processing steps and included in the output products, so that a complete history of error estimates and data quality (DQ) flags is preserved. After this step is performed, the science data are in the same form as the raw science data from any other observing mode and are processed the same way throughout the remaining steps of **calnica**. No reference files are used by this step.

Figure 16.2: Partial NICMOS Header

```
                / CALNICA CALIBRATION REFERENCE FILES

MASKFILE= 'nref$h4214599n_msk.fits' / static data quality file
NOISFILE= 'nref$h4216218n_noi.fits' / detector read noise file
NLINFILE= '/data/mimir2/eddie/7116/customlin.fits'
DARKFILE= '/data/mimir2/eddie/darkplace/c2_step256_med.fits'
FLATFILE= '/data/mimir2/eddie/flatplace/c2_f110w_new.fits'
PHOTTAB = 'nref$h1t0826ln_pht.fits' / photometric calibration table
BACKTAB = '                    ' / background model parameters table

                / CALNICA CALIBRATION REFERENCE FILE PEDIGREE

MASKPDGR= 'GROUND 15/01/1997'  / static data quality file pedigree
NOISPDGR= 'GROUND 27/01/1997'  / detector read noise file pedigree
NLINPDGR= 'GROUND 27/01/1997'  / detector nonlinearities file pedigree
DARKPDGR= 'INFLIGHT 10/03/1997'/ dark current file pedigree
FLATPDGR= 'GROUND 15/01/1997'  / flat field file pedigree
PHOTPDGR= 'GROUND 17/10/1996'  / photometric calibration table pedigree
BACKPDGR= '                    ' / background model parameters table pedigree

                / CALNICA CALIBRATION SWITCHES: perform,omit

BIASCORR= 'PERFORM             ' / subtract ADC bias level
ZOFFCORR= 'PERFORM             ' / subtract MULTI-ACCUM zero read
MASKCORR= 'PERFORM             ' / data quality initialization
NOISCALC= 'PERFORM             ' / calculate statistic errors
NLINCORR= 'PERFORM             ' / correct for detector nonlinearities
DARKCORR= 'PERFORM             ' / dark correction
FLATCORR= 'PERFORM             ' / flat field correction
UNITCORR= 'PERFORM             ' / convert to count rates
PHOTCALC= 'PERFORM             ' / calculate photometric keywords
CRIDCALC= 'PERFORM             ' / identify cosmic ray hits
BACKCALC= 'PERFORM             ' / calculate background estimates
WARNCALC= 'OMIT    '             / generate user warnings

                / CALNICA CALIBRATION INDICATORS: performed, skipped, omitted

BIASDONE= 'PERFORMED'            / subtract ADC bias level
ZOFFDONE= 'PERFORMED'            / subtract MULTI-ACCUM zero read
MASKDONE= 'PERFORMED'            / data quality initialization
NOISDONE= 'PERFORMED'            / calculate statistic errors
NLINDONE= 'PERFORMED'            / correct for detector nonlinearities
DARKDONE= 'PERFORMED'            / dark correction
```


MASKCORR

Flag values from the static bad pixel mask file are added to the DQ image. This uses the MASKFILE reference file, which contains a flag array for known bad (hot or cold) pixels. There is one MASKFILE for each detector.

BIASCORR

NICMOS uses 16-bit analog-to-digital converters (ADCs), which convert the analog signal generated by the detectors into signed 16-bit integers. Because the numbers are signed and because the full dynamic range of the converter output is used, raw pixel values obtained from individual detector readouts can range from –32768 to +32767 DN. In practice the detector bias level is set so that a zero signal results in a raw value on the order of –23000 DN. In ACCUM, BRIGHT OBJECT, and RAMP modes, where the difference of initial and final readouts is computed on-board, the subtraction is also performed in 16-bit arithmetic. Therefore, it is possible that the difference between the final and initial pixel values for a bright source could exceed the dynamic range of the calculation, in which case the final pixel value will wrap around the maximum allowed by the 16-bit arithmetic, resulting in a negative DN value. Given the level at which the

Figure 16.3: Pipeline Processing by CALNICA

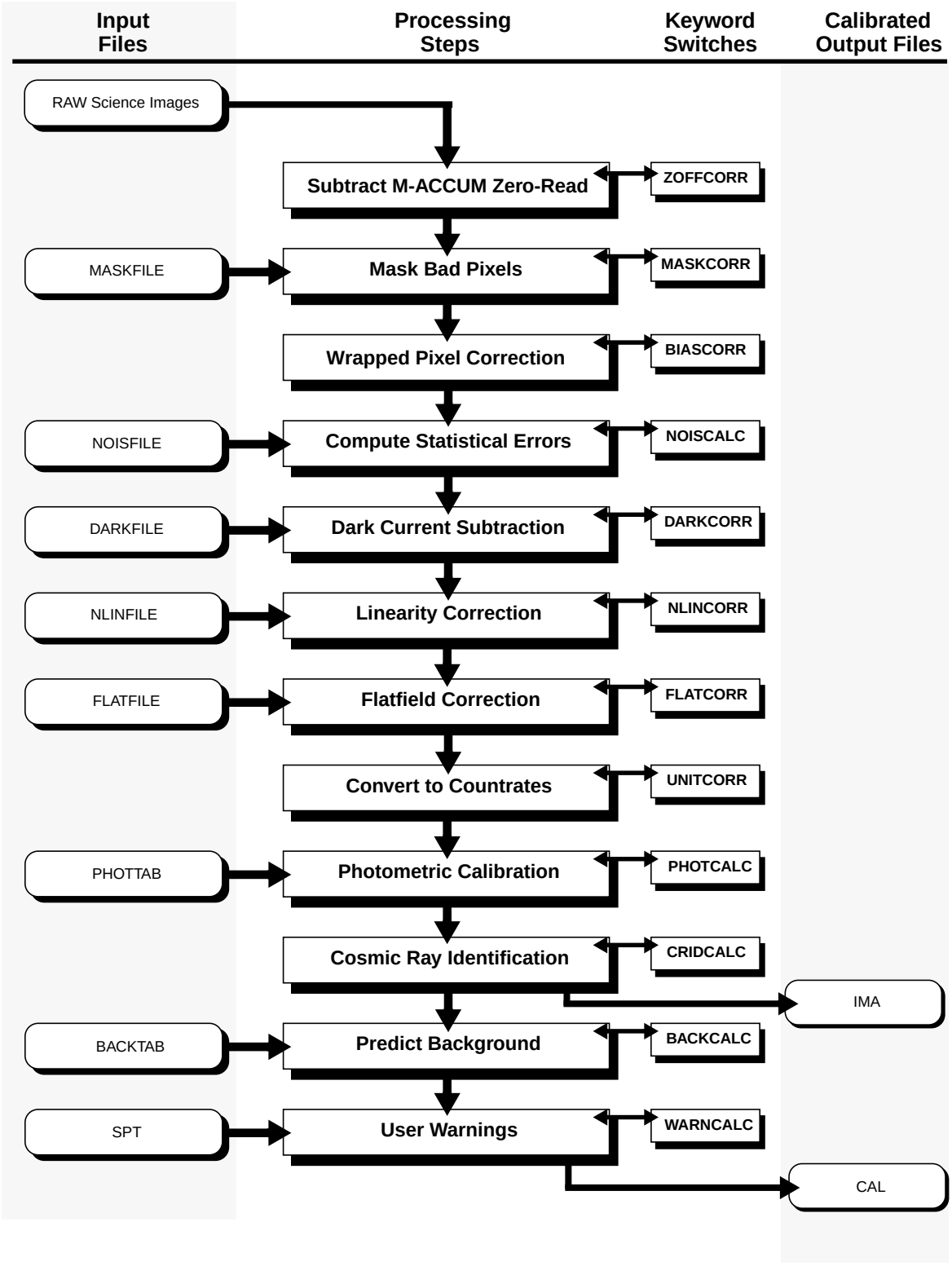

NICMOS detectors saturate, and the analog-to-digital conversion factor, the maximum “real” pixel value that is expected is on the order of +40000 DN. Such a value will be wrapped to about –26000 DN by the on-board difference calculation.

The BIASCORR step therefore searches for pixel values in the range –26000 to –32768 and adds an offset of 65536 DN to these pixel values to reset them to their original real values.

No reference files are used by this step.

NOISCALC

NICMOS calculates statistical errors for the science data only in the RAMP observing mode. Errors for all other modes are computed in the **calnica** pipeline. The NOISCALC step performs the task of computing an estimate of the errors associated with the raw science data based on a noise model for each detector. Currently the noise model is a simple combination of detector read noise and Poisson noise in the signal, such that:

$$\sigma = \frac{\sqrt{\sigma_{rd}^2 + \text{counts} \cdot \text{adcgain}}}{\text{adcgain}} \qquad \text{Eq. 16.1}$$

where σ_{rd} is the read noise in units of electrons, *adcgain* is the analog-to-digital conversion gain factor (in electrons per DN) and *counts* is the signal in a pixel in units of DN. Noise is computed in units of electrons, but the result is converted to units of DNs for storage in the error image. The detector read noise is read pixel-by-pixel from the NOISFILE reference image and depends on the read rate of the observation, as well as the number of initial and final reads (NREAD). Separate NOISFILEs are required for each combination of read rate and NREAD. The data quality flags set in the DQ image of the NOISFILE are propagated into the DQ images of all image sets (imsets) being processed.

For RAMP mode observations, the error estimate computed by the instrument (and therefore, present in the raw science file) is a variance. For these observations the NOISCALC step simply computes the square-root of the raw error image so that it is on the same basis as other modes.

Throughout the remaining steps in **calnica**, the error image is processed in lock-step with the science image, getting updated as appropriate. Errors are mostly propagated through combination in quadrature.

DARKCORR

The detector dark current is removed from the science image by subtracting a dark current reference image appropriate for the exposure time of the science data.

A simple scaling of a single dark reference image to match the exposure time of the science data is, unfortunately, not possible due to the non-linear behavior of the dark current as a function of time. Therefore, a library of dark current images is maintained, covering the range of exposure times of the MULTIACCUM sequences and a subset of ACCUM exposure times and NREAD values (see the *NICMOS Instrument Handbook*). The reference dark appropriate for the exposure time and sequence used in MULTIACCUM, or the exposure time and NREAD values used in ACCUM, is determined and subtracted from the data. For

non-standard MULTIACCUM sequences (see the *NICMOS Instrument Handbook*) and for some ACCUM exposure times, the appropriate dark image is interpolated from existing dark files. There is one reference file (DARKFILE) per detector, which contains the set of dark images (at various exposure times) for that detector. Error estimates of the dark current, stored in the ERR images of the DARKFILE, are propagated in quadrature into the ERR images of all processed IMSETs. Data quality (DQ) flags set in the DARKFILE are also propagated into the DQ images of all processed imsets.

Sets of synthetic dark reference files have been recently generated to populate the calibration database. These dark files reproduce all the characteristics of on-orbit darks, which do not suffer from the *pedestal* (see Chapter 17).

Dark subtraction is skipped in BRIGHTOBJ mode, because the short exposure times should result in insignificant dark current.

NLINCORR

The linearization correction step corrects the integrated counts in the science image for the non-linear response of the detectors. The observed response of the detectors can conveniently be represented by 3 regimes:

- At low signal levels the response is linear and no correction is needed; the low signal level for NICMOS is pixel- and camera-dependent, and is about 14,500 DN and below, with a standard deviation of about 400 DN.
- At intermediate levels the detector response deviates in a linear fashion from the incident flux and is easily correctable via the expression:

$$F_c = (c1 + c2 \times F) \times F$$

  where *c1* and *c2* are the correction coefficients, *F* is the uncorrected flux (in DN) and F_c is the corrected flux.
- At high signal levels—as saturation sets in—the response becomes highly non-linear and is not correctable to a scientifically useful degree; the saturation level is about 30,500 DN, with a standard deviation of about 2,000 DN.

The NLINCORR step applies no correction to pixels in the low signal regime, applies a linear correction term to intermediate level pixels, and applies no correction to pixels in the high signal regime but rather flags them in the DQ image as saturated. This step uses the NLINFILE reference file, which consists of a set of images containing correction coefficients and variances at each pixel. Error estimates on the correction applied to intermediate-level pixels are propagated into the ERR images of all imsets processed. Data quality flags set in the NLINFILE are also propagated into the processed DQ images. There is one NLINFILE per detector.

FLATCORR

In this step the science data are corrected for variations in gain between pixels by multiplying by an (inverse) flatfield reference image. This step is skipped for

observations using a grism because the flatfield corrections are wavelength dependent. This step uses the FLATFILE reference file, which contains the flatfield image for a given detector and filter (or polarizer) combination. Error estimates and DQ flags contained in the FLATFILE are propagated into the processed images. There is one FLATFILE per detector and filter combination.

UNITCORR

The conversion from raw counts to count rates is performed by dividing the science and error image data by the exposure time. No reference file is needed.

PHOTCALC

This step provides photometric calibration information by populating the photometry keywords PHOTMODE, PHOTFLAM, PHOTFNU, PHOTZPT, PHOTPLAM, and PHOTBW with values appropriate to the camera and filter combination used for the observation. The photometry parameters are read from the PHOTTAB reference file, which is a FITS binary table containing the parameters for all observation modes. The values of PHOTFLAM and PHOTFNU are useful for converting observed count rates to absolute fluxes in units of erg/s/cm^2/Angstrom or Jy, respectively.

CRIDCALC

This step identifies and flags pixels suspected of containing cosmic ray (CR) hits. For MULTIACCUM mode observations, this step also combines the data from all readouts into a single image. In MULTIACCUM mode, the data from all readouts are analyzed pixel-by-pixel, searching for and identifying the data from individual readouts that appear as outliers using an iterative sigma-clipping technique. In each pixel, the signal from each readout is ascribed a standard deviation given by the combination of readnoise and Poisson noise. Values which deviate more than 5 σ from the mean slope of the counts-versus-time relation are identified as outliers, and the corresponding pixels in the DQ images of the intermediate MULTIACCUM (*_ima.fits) file are flagged, however, the pixel values themselves in the SCI and ERR images are unchanged. Once all outliers have been identified, a final, combined value is computed for each pixel using only non-flagged samples. The result of this operation is stored as a single imset in the output *_cal.fits file in which the number of unflagged samples used to compute the final value for each pixel and the total exposure time of those samples will be reflected in the SAMP and TIME images. The variance ascribed to the final mean countrate is the uncertainty in the slope of the counts-versus-time relation at each pixel location. Pixels for which there are no unflagged samples, e.g., permanently hot or cold pixels, will have their output SCI, ERR, SAMP, and TIME values set to zero, with a DQ value that contains all flags that were set. The cosmic ray rejection threshold, 5 σ, is currently hardwired in the **calnica** code, and seems to perform a reasonable job of identifying and rejecting cosmic rays.

The algorithm is not yet completely defined or implemented for ACCUM, BRIGHTOBJ, and RAMP mode observations, therefore the *_cal.fits output file for these modes will still contain cosmic ray hits.

BACKCALC

This step computes a predicted background (sky plus thermal) signal level, based on models of the zodiacal scattered light and the telescope plus instrument thermal background. This step uses the BACKTAB reference table which contains the background model parameters. Results are written to the BACKEST1, BACKEST2, and BACKEST3 header keywords. The image data are not modified in any way. This step is not yet implemented.

WARNCALC (User Warnings)

In this step various (as yet undetermined) engineering keyword values are examined and warning messages are generated if there are any indications that the science data may be compromised due to unusual instrumental characteristics or behavior. This step is not yet implemented.

16.4 Mosaicing: Calnicb

Observing strategies with NICMOS vary according to the nature of the target object and of the wavelength chosen for the observation. Extended objects may require mosaicing. Long wavelength observations will need chopping onto the sky to remove the telescope thermal background from the target frame. Multiple repetitions of the same exposure may be requested to improve cosmic ray removal, to control statistical fluctuations, and to increase the signal-to-noise on one target while avoiding saturation on another. Dither (mosaicing) and chop patterns of exposures are specified at the Phase II proposal level via the optional PATTERN parameter; multiple exposures at the same pointing are specified in Phase II by setting the Number_of_iterations to a value greater than one. All these options (which can also be set simultaneously) create an *association* of datasets (see “Associations” on page B-4).

The **calnicb** task (Figure 16.4) produces the combined, or *mosaiced*, image from the multiple images contained in a NICMOS association. The task also performs background subtraction and source identification on the images in the association.

Figure 16.4: Conceptual calnicb Pipeline

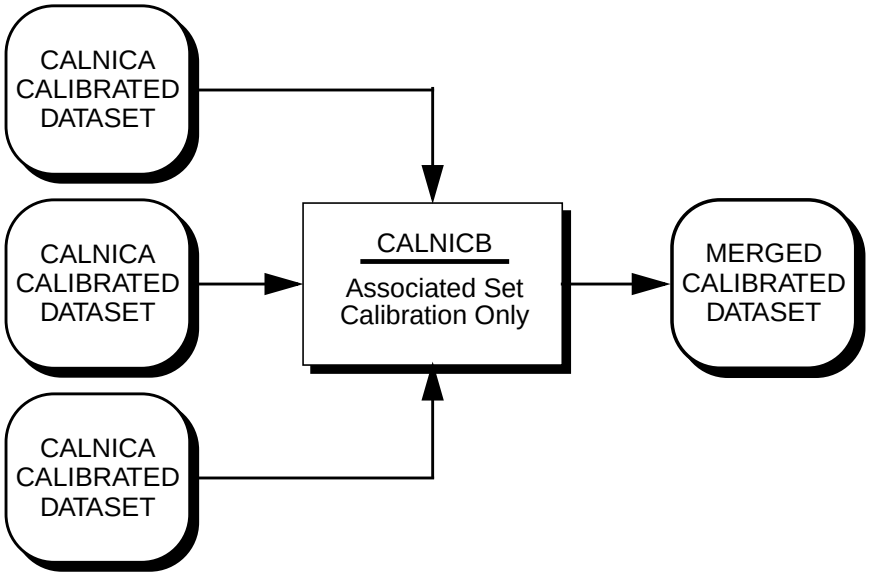

16.4.1 Input Files

Two levels of input data are needed by **calnicb**:

1. The *association table* (*assoc_id*_`asn.fits`): this is a table containing three columns with the list of members in the association and the relevant information on the association type, as given in Table 16.1.

Table 16.1: Columns of the Association Table (input to calnicb):

Column Name	Meaning
MEMNAME	Rootname (*IPPPSSOOT*) of each image in the association.
MEMTYPE	Role or type of each member: EXP-TARG = input exposure for target EXP-BCK*n* = input exposure of *n*-th background (for chop patterns) PROD-TARG = output product containing target PROD-BCK*n* = output product containing n-th background (for chop patterns)
MEMPRSNT	Flag indicating whether or not a member is present (needed by the STScI automatic pipeline processing).

The header of the *assoc_id*_`asn.fits` table also contains the setting of the keywords which control the background illumination pattern correction (ILLMCORR); the keywords read are: ILLMCORR (whether or not the correction must be performed) and ILLMFILE (reference file name for the illumination correction); these are explained in Chapter 15. At the time of

this writing (August 1997) we have not been able to measure any such spatial variations, and the ILLMFILEs have not yet been populated.

2. The input images (*ippssoot*_cal.fits): the science data images which are part of the association, as listed in the first column of the association table. The images are usually the calibrated outputs of **calnica**.

3. The support files (*ipppssoot*_spt.fits), containing the engineering information, so that calnicb can transfer this information to the output support files.

16.4.2 Output Files

Calnicb produces two levels of outputs:

1. An updated copy of the association table (*assoc_id*_asc.fits): this copy of the *assoc_id*_asn.fits file contains additional information about the processing that took place. The *assoc_id*_asc.fits file contains four additional columns, listed in Table 16.2.

Table 16.2: Additional Columns of the output Association Table:

Column Name	Meaning
BCKIMAGE	Flag indicating whether or not the image was used to compute the background.
MEANBCK	Values of the mean background for the image (DN/sec).
XOFFSET	X-offset (in pixels) of the image from the reference frame; a positive value means a positive offset of the image (not of the sources) relative to the reference.
YOFFSET	Y-offset (in pixels) of the image from the reference frame; a positive value means a positive offset of the image (not of the sources) relative to the reference.

Additional information contained in the header of the *assoc_id*_asc.fits table is the MEAN_BCK keyword, which gives the constant background signal level subtracted from all images in the association.

2. One or more output mosaic images (*assoc_idn*_mos.fits): the number of output mosaic images depends on the pattern. The target field is always contained in the *assoc_id*0_mos.fits file. Patterns which involve chopping onto the sky to produce background reference images result in multiple *assoc_idn*_mos.fits files after processing through **calnicb**. In these cases, the target is still contained in the *assoc_id*0_mos.fits file; for each background position an additional mosaic, *assoc_id*n_mos.fits with *n*=1 to 8, is created.

3. One *assoc_id*_spt.fits support file for each *assoc_id*_mos.fits file created.

16.4.3 Processing

The basic philosophy of the **calnicb** algorithm is to remove the background from each image after source identification, to align the images by calculating offsets, and to produce the final mosaic. The processing steps of **calnicb** can be summarized as follows:

1. Read the input `asn` table and input images.
2. Determine processing parameters from keyword values.
3. Combine multiple images at individual pattern positions.
4. Identify sources in the images.
5. Estimate and remove the background signal.
6. Create a mosaic image from all pattern positions.
7. Write the output association table and mosaic images.

The sections below discuss steps 2 through 6 in greater detail.

Processing Parameters

Header keywords from the input `*_cal.fits` images are read and evaluated in order to guide the processing. One set of keywords (Table 16.3) pertains to the association as a whole and therefore are read only once from the first input member image.:

Table 16.3: Common Keywords to all Association Datasets

Keyword	Purpose
INSTRUME	Check whether they are NICMOS data.
CAMERA	Camera number.
FILTER	Filter; if BLANK, the association is made of darks.
IMAGETYP	Type of image (EXT=external, DARK=dark frames, FLAT=flat-field images).
NUMITER	Number of iterations for each exposure.
PATTERN	Pattern used.
NUMPOS	Number of independent positions in the pattern.

A second set of header keywords (Table 16.4) are specific to each member of the association, and must be read from each single input image.:

Based on this information, an inventory is taken of what input images exist, where they belong in the pattern, how many there are at each pattern position, which images are from the target field, which ones are from background fields, and which output mosaic image each input image will eventually end up in. As part of the input process, the appropriate ILLMFILE reference file is loaded.

Table 16.4: Dataset-specific Keywords

Keyword	Purpose
PATT_POS	Position of the image in the pattern.
BACKEST*n*	Background estimates from **calnica.**
CRPIX*n*, CRVAL*n* CD*n_n* CTYPE*n*	World Coordinate System (WCS) information (see Table 15.5).

Combination of Multiple Exposures

If there is more than one image at any pattern position (NUMITER > 1), the multiple images at each position are first registered and then combined into a single image. The coordinates (as determined by the WCS keywords) of the first image at a given pattern position are used as a reference for the registration. The offsets to all other images at that pattern position are first computed by comparing their WCS data, and then refined using a *cross-correlation* technique**,** down to a level of 0.15 pixels. The cross-correlation technique employes an algorithm which minimizes the differences between fluxes in the images. The computed offsets, in units of pixels, are recorded in the output association table. After determining the relative offsets, the images are aligned using *bilinear interpolation* and are then combined on a pixel-by-pixel basis. The combined pixel values are computed as a weighted mean of all unflagged (i.e., DQ = 0) samples, using the input image ERR values as weights. If three or more samples are present, iterative σ-clipping is performed to reject outliers. The number of samples used at each pixel and the total integration time are retained.

Source Identification

The source identification step is used for excluding sources when the background in the images at each pattern position is estimated. The images at each pattern position are searched for pixels suspected to contain signal from a source. The mean signal level in the image is computed and pixels that are more than 3 σ above the mean are searched for. Spurious results, such as pixels containing cosmic-ray hits, are filtered out by searching neighboring pixels and only retaining those that have two or more neighbors that are also above the threshold. The DQ flag of the source-affected pixels is then set to 1024.

Background Estimation and Removal

The background signal is estimated and removed from the images at each pattern position. Two types of background are subtracted from the images:

1. A *constant background* signal level, which is estimated from the images themselves.
2. The two-dimensional residual signal that may exist due to spatial variations in the thermal emission of the telescope and instrument; this is removed by subtracting the ILLMFILE reference image from each image (this second step can be turned on or off via the ILLMCORR keyword in the association table header). At the time of this writing (August 1997) we have not been

able to measure any such spatial variations, and the ILLMFILEs have not yet been populated.

The *constant background* signal level is estimated and removed as follows.

1. With chop patterns, the mean and standard deviation of the signal in the image at each chop position is computed. In addition to excluding bad and source-flagged pixels, the calculation of the mean also uses iterative σ-clipping to reject outliers.
2. With dither-only patterns, or with multiple-exposure single pointings, the mean and σ of the target images is computed. The result for each image is compared to the estimate provided by **calnica**, which is stored in the BACKEST1 header keyword of each image. The value computed by **calnicb** is accepted if it is less than 5 σ deviant from that of **calnica**, otherwise the **calnicb** value is assumed to be biased by the presence of sources and the **calnica** value is substituted for it.
3. The global mean and standard deviation of the background is computed from the values of each image, using iterative σ-clipping to reject outliers.
4. The final mean background value is subtracted from all images (both target and background images, if present).

Mosaic Construction

Mosaic (MOS) images are created for each independent pointing within the pattern. For example, a combination DITHER-CHOP pattern will produce one mosaic image out of the dithered pattern at each CHOP location on the sky. Each mosaic image is created as follows:

1. The relative offsets between images within the mosaic are computed from their WCS information and refined using cross-correlation (as in the case of multiple exposures at each pattern position, see above). The first image in the list for each mosaic is used as a reference image.
2. An empty mosaic image is created with *x* and *y* dimensions large enough to encompass the maximum offsets in each direction.
3. Pixel values in the mosaic image are computed by combining samples from overlapping images. The individual images are aligned using bilinear interpolation and the value at a given mosaic pixel location is computed from the error-weighted mean of the samples at that location. Samples flagged as bad are excluded and, if three or more samples are present, iterative σ-clipping is used to reject remaining outliers. The number of samples retained for a given pixel and their total integration time is recorded in the SAMP and TIME images. If all samples are rejected for a pixel, the mosaic image SCI, ERR, SAMP, and TIME values are set to zero and a combination of all DQ flags is retained.

16.5 Grism Data Reduction: Calnicc

Calnicc is an IDL program designed for the automatic extraction of spectra from NICMOS multi-object grism images. The basic capabilities of the program are the following. Objects are identified on a direct image and classified as stars or galaxies using a neural network approach implemented as the SExtractor program (Bertin and Arnouts, 1996, *A & A Suppl.* 117, 393). The positions of the objects are used to extract spectra from a grism image of the same region. After extraction, the spectra are wavelength calibrated, flat-fielded, and flux calibrated. The extracted spectra are corrected for contamination from nearby objects. Subsequently, the extracted spectra are automatically searched for emission and absorption lines, and the continuum level of each spectrum is determined. Figure 16.5 shows the flow chart for **calnicc**.

16.5.1 Input Files

Calnicc expects two input files:

- *Direct image* of the target field (`*_cal.fits`); the image has been typically obtained with one of the NICMOS continuum filters, possibly at a wavelength within the range covered by the grism. The direct image given as input to **calnicc** is the calibrated output file of **calnica**.
- *Grism image* of the target field (`*_cal.fits`); this image has also been processed by **calnica**. By default, **calnica** does not flat-field grism images, because the flat-field is wavelength dependent and must be applied to the final extracted spectra. **Calnicc** provides the flat-fielding step.

16.5.2 Output Files

A number of outputs are generated by **calnicc**:

1. A FITS table containing the extracted spectra (*image*`_tab.fits`). This file contains the successfully extracted spectra; it consists of a primary header and a series of table extensions, each extension consisting of a header and the associated table. There is one table extension for each spectrum extracted. The primary header of the file contains the relevant information regarding the observation, namely a subset of the keywords in the primary headers of the input direct and grism images. The table extension header contains keywords relevant for the individual spectrum; the keywords describe: the content of the table (the list of columns), the nature and position of the object, and the characteristics of the spectrum (line positions and fluxes, continuum level, etc.). The associated table contains five columns: the wavelength vector, the flux vector, and three vectors of the statistical, deblending, and total errors from the extraction process.

Figure 16.5: Flowchart of calnicc Processing

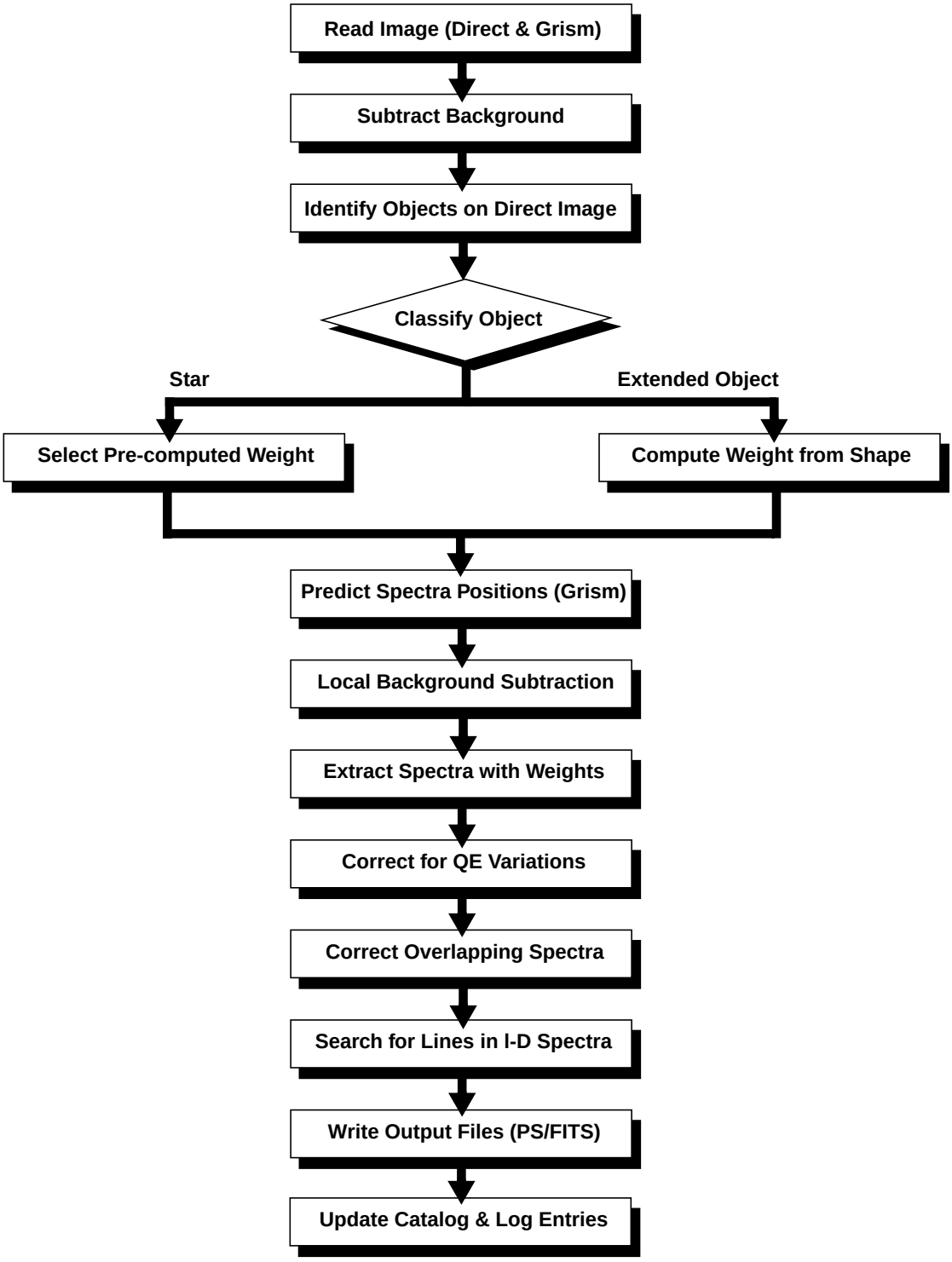

2. Postscript files of the extracted spectra (*image_n*.ps). The files contain graphical representations of the extracted spectra. One postscript file for each spectrum is generated, where n is a sequential number starting with 0.
3. Background image (*image*_po.fits). This file is equivalent to the original grism image, except that all pixels used in the spectra extraction are replaced by the surrounding background level.
4. Background identification image (*image*_bg.fits). This is an image where the pixels used in the background estimate calculation are highlighted.
5. The catalog of objects (calnicc.cat). This is a list of all the objects whose spectrum has been successfully extracted. For each object the catalog reports information about its position, nature, and characteristics of the extracted spectrum.
6. The log file (calnicc.log). The log file contains statistics on the **calnicc** processing.

16.5.3 Processing

Calnicc was developed using the Interactive Data Language (IDL) software. However the C program **SExtractor** (Bertin and Arnouts, 1996) is used for source object detection. Below a brief description of the algorithms used at each step of the processing is given, following the basic outline of the flow chart in Figure 16.5.

Object Detection and Classification

After both the direct and grism images have been read by the program, **calnicc** checks whether there is a background estimate in the header of the *_cal.fits images and subtracts it from the data, if present.

A third-party program, **SExtractor** is used then to detect and classify (point-like or extended) objects on the direct image. This program is thoroughly documented in the *SExtractor 1.0 User's Guide*. **SExtractor** does not use the data quality flags or the error arrays to perform the detection, and spurious objects may be introduced in the catalog. To remove spurious detections, the pixels where the object lies are compared to the quality flag array. If the ratio of bad pixels to the total number of pixels used by the object is above a user-defined threshold, the object is considered as spurious and not processed any further. In addition, the total flux within any object is compared to the quadratic sum of the error estimates for the individual pixels within the object. Again, a user supplied threshold for the significance is used to remove spurious or weak objects.

The grism images are also searched for additional sources. Grism images may yield objects which are located outside of the detector (and therefore are not present in the direct image), but have part of the spectrum on the grism image. Or objects which have most of the flux contained in a single spectral line; in this case, the usually short exposure time of the direct image might not be enough to detect the object, while the typically longer exposure time of grism image may allow the

detection. The grism image is prepared by replacing pixels used by previously detected objects' spectra with the background level. Subsequently, DAOFIND is used to find objects more than DAOTHRESH x σ above the background, where σ is the rms of the image after removing the spectra. Since no zero point for the wavelength scale is known for those spectra, the objects' location is simply noted in the log file, but no attempts are made to extract their spectra.

Background Subtraction

After source identification, an estimate of the two-dimensional background level is derived and removed from each image.

The grism image is not flat-fielded and the QE variations across the NICMOS detectors are strong, implying that a significant structure is present in an image of blank sky. The QE variations depend significantly on the wavelength, and the expected background in the grism image will depend on the spectrum of the background in space. The present version of **calnicc** uses a pre-computed model of the background in space, which will be replaced by measures of the blank sky when these data become available. The model used for the background estimate includes three different thermal sources:

- Thermal radiation from the HST itself.
- Thermal radiation from the NICMOS optics.
- Near infrared zodiacal emission.

These three components and their wavelength dependence are discussed in the *NICMOS Instrument Handbook*.

The model background image for each grism is stored in an associated background FITS file. This image is scaled to the local flux within a region around each spectrum on the grism image, and the rescaled background is subtracted from the image itself. The scaling factor is calculated by taking the mean flux values of an ellipsoidal region surrounding each spectrum (but excluding the spectrum itself), and dividing it by the mean of the background image in the same region. Pixels belonging to overlapping spectra from two or more objects are excluded from the computation of the scaling factor. The uncertainty in the background estimate is given by the square root of the sum of the errors divided by the square root of the number of pixels.

Spectra Extraction

Wavelength Calibration

Both the dispersion relation and the deviation of the spectra from a straight line (distortion) are parametrized as third degree polynomials. The coefficients of the polynomials and the orientation of the spectra relative to the direction of the rows are contained in the reference file `grismspec.dat`. The dispersion relation is given by:

$$\lambda = a_0 + a_1 x + a_2 x^2 + a_3 x^3 \qquad \text{Eq. 16.2}$$

where x is the deflection in pixels relative to the position of the object in the direct image and λ is the corresponding wavelength.

The distortion of the spectra is parameterized as:

$$\Delta y = b_0 + b_1 r + b_2 r^2 + b_3 r^3 \qquad \text{Eq. 16.3}$$

where r is the distance of a pixel (x,y) from the object of coordinates (x_o, y_o) and Δy is the deviation in pixels of the spectrum from a horizontal line. The alignment of the spectrum is taken into account by rotating the grism image around the object position (x_o, y_o) prior to the extraction. The distortions in the spectra are taken into account by introducing a corresponding distortion in the weights used for the extraction.

Flux and Error Bars

Once objects on the images have been detected, their spectra can be extracted. Extraction of spectra is accomplished by using a weight matrix to calculate the flux vector for each wavelength. The flux is then given by:

$$F_j = \sum_i w_{ji} g_{ji} \qquad \text{Eq. 16.4}$$

where the sum over the flux g_{ji} of all pixels at wavelength λ is performed with weights w_{ji}. The weights used to compute the spectra depend on the size of the objects. Two scenarios are handled by **calnicc**: point sources and extended objects (e.g., galaxies). For point sources, the weights are computed from simulated PSFs generated via the TinyTim software. The weights are optimal for point sources with flux-independent noise, namely, background dominated. For extended objects, the weight matrix is built from the direct image, under the assumption that the shape of the object is independent of wavelength. The size and orientation of the object is computed from the direct image using the moments of the image. The weight matrix is then created by summing up all the pixel values in a given row (fixed wavelength) of the grism image that fall within the ellipse defined by the size and orientation the object in the direct image.

The error estimate ε_{ji} for each pixel is taken from the ERR array of the input grism image. The error estimate ε_j for each wavelength is then the weighed quadratic sum over the errors of all pixels at constant wavelength.

Flatfielding of Spectra

After the spectra are extracted, the fluxes are corrected for the variations of the quantum efficiency of the detector (flatfielded). The QE variations depend both on the wavelength and on the position of the object on the detector. Because of this wavelength dependence, the flatfielding cannot be performed before the spectra are extracted. The correction factors are derived through interpolation from a set of monochromatic flatfield images stored as a single FITS file called `nicmosFF.fits`.

Deblending of Overlapping Spectra

Since the NICMOS grisms are slitless, overlaps among different spectra are likely to happen. The strategy of observing the same target at different telescope roll angles helps removing overlap in many instances. In addition, **calnicc** has been designed to *deblend* the spectra—to remove or minimize contamination of one spectrum from another.

The deblending algorithm is described in detail in the **calnicc** manual. The basic requirement for the algorithm to work is that, at each wavelength, different spatial portions of the spectrum to be deblended have different levels of contamination. The deblending algorithm relies on the assumption that the shape of the object is the same at all wavelengths. The deblending procedure produces also an error estimate which is reported in the output FITS table and indicated in the postscript file containing the spectrum.

16.6 Recalibration

This section is intended to help you decide whether your data were calibrated with optimal calibration reference files and to help you decide whether you need to recalibrate your data.

16.6.1 Why Recalibrate?

Many users will find that the calibrated data produced by the OPUS pipeline—the standard calibration—are adequate for most scientific applications. The **calnica** pipeline calibrated your data with the most up-to-date, instrument configuration-specific reference files available at the time of the observation. However, updated or timely reference files sometimes do become available after your data were processed. Improved software for calibration (both **calnica** and **calnicb**) may also become available as our understanding of the instrument performance increases with on-orbit experience. This is especially true for data obtained during the first few months of the NICMOS lifetime in orbit. Particularly if you notice unusual features in your data, or if your analysis requires a high level of accuracy, you may wish to determine whether a better set of calibration reference files exist than were used to process your data. If better files are available or the calibration software changes significantly, you may choose to recalibrate your data using the new files or software.

Finding that a calibration reference file has changed since your data were calibrated doesn’t always mean that you have to recalibrate. The decision depends very much on which calibration image or table has changed, and whether that kind of change to your data is likely to affect your analysis in a significant way. Before deciding to recalibrate, you might want to retrieve the new recommended reference file or table and compare it to the one used to calibrate your data at STScI in order to determine if the differences are important. You can use the table tools in the STSDAS **ttools** package to manipulate and examine calibration tables; images can be manipulated in the same way as your science data.

16.6.2 Recalibrating the Data

This section describes the mechanics involved in actually recalibrating a dataset. The basic steps in recalibrating a dataset are:

1. Assemble any necessary reference files or tables and your raw data files.
2. Set the desired calibration switches and reference file name keywords in the *primary header* of your raw (`*_raw.fits`) data file. These determine which steps will be executed by the calibration software and which reference files will be used to calibrate the data.
3. Run the calibration software.

Assembling the Input Files

In order to recalibrate your data, you need to retrieve *all* of the reference files and tables that are used by the calibration steps you want to perform. The source of these files is the Calibration Database (CDBS) at STScI. A complete description of how to retrieve the reference files is given in Chapter 1.

Setting the Calibration Parameters

The calibration software is completely data-driven, meaning that the calibration steps to be carried out are determined by the values of the *calibration switches* and the *calibration reference files* keywords contained in the primary header of the file to be processed. An important step is then to set the calibration switches and reference file keywords in the primary header of your raw data file (`*_raw.fits`) to reflect how you want the data recalibrated and which reference files you want to use at each step in the process. This is done most easily with the **chcalpar** task in the **hst_calib.ctools** package of STSDAS or with the **hedit** task in the IRAF **images** package.

The calibration switch keywords reside only in the primary header of NICMOS FITS files: it is critically important to *specify extension number zero explicitly* when passing file names to tasks like **chcalpar** or **hedit** to modify these keywords. For example, to modify calibration keywords in the file `n3xe01bhm_raw.fits`, be sure to use the complete name `n3xe01bhm_raw.fits[0]` as input to these tasks. If you do not specify extension zero explicitly, the keywords you modify will end up getting written into the first extension header instead, where **calnica** will *not* find them.

The **chcalpar** task takes a single input parameter—the name(s) of the raw data files to be edited. When you start **chcalpar**, the task automatically determines that the image data are from NICMOS and opens a NICMOS-specific parameter set (*pset*) that will load the current values of all the calibration-related keywords. To edit the calibration keyword values:

1. Start the **chcalpar** task, specifying the image(s) in which you want to change keyword values. If you specify more than one image, for example using wildcards, the task will read the initial keyword values from the first

image in the list. For example, you could change keywords for all NICMOS raw science images in the current directory (with initial values from the first image), using the command:

```
ct> chcalpar n*raw.fits
```

An example of using **chcalpar** on a single NICMOS file is shown in Figure 16.6.

2. After starting **chcalpar**, you will be placed in **eparam**—the IRAF parameter editor, and will be able to edit the set of calibration keywords. Change the values of any calibration switches, reference files or tables to the values you wish to use for recalibrating your data.

3. Exit the editor when you are done making changes by typing `:q` two times. The task will ask if you wish to accept the current settings. If you type “y”, the settings will be saved and you will return to the IRAF `cl` prompt. If you type “n”, you will be placed back in the parameter editor to redefine the settings. If you type “a”, the task will abort and any changes will be discarded.

Figure 16.6: Editing Calibration Keywords with chcalpar

Running the Calibration Software

After you change the header keyword values for your raw data files, you are ready to recalibrate your data. To run **calnica**, type the name of the task followed by the names of the input raw data file and desired output calibrated data file. For example, to recalibrate the dataset `n0g70106t`, you could type:

```
ni> calnica n0g70106t_raw.fits n0g70106t_cal.fits
```

or:

```
ni> calnica n0g70106t “ “
```

To run **calnicb** the name of the association table must be given as input:

```
ni> calnicb assoc_id_asn
```

To run **calnicb** on a subset of the `*_cal.fits` files, it is sufficient to edit the `*_asn.fits` table and remove the undesired files.

The calibration routines **calnica** and **calnicb** will not overwrite an existing output file. If the calibration tasks are run in the directory where the original calibrated files are located, a different output file name must be specified.

16.6.3 Calculating Absolute Sensitivity

The PHOTCORR step in **calnica** does not alter the values of the data (which are always in countrates in the calibrated file), but only writes the information necessary to convert countrates to fluxes into the header of the file, i.e., sets the values of PHOTFLAM, PHOTFNU, PHOTPLAM, PHOTBW, PHOTZPT, and PHOTMODE. Unless you wish to recalculate the absolute sensitivity for your observation (e.g., because a more recent throughput estimate exists for your observing mode), there is no need to recompute these values and you can set `PHOTCORR=OMIT` in the recalibration.

Chapter 17
NICMOS Error Sources

In This Chapter...

This chapter describes the most common sources of uncertainty affecting calibrated NICMOS data. Some of these will be propagated into the Error Array of the calibrated data (e.g., flatfield uncertainties) or into the Data Quality Array (e.g., grot and hot pixels). These sources all represent limiting factors for the sensitivity of the NICMOS observations. In addition, some error sources found during the Science Mission On-orbit Verification (SMOV) are described (e.g., non-zero zeroth read, dark current pedestal), to help observers decide whether their data need to be recalibrated or analyzed with particular care.

Many details in this chapter are based on preliminary results from the SMOV, and will evolve as our understanding of the on-orbit NICMOS performace improves. Updates will be periodically posted on the NICMOS WWW pages.

17.1 Flatfield Errors

17.1.1 Thermal-Vacuum versus On-Orbit Flatfields

A full set of flatfield frames was taken with the NICMOS arrays during the System Level Thermal Vacuum test, conducted on the ground in August 1996. However, because of the thermal short experienced by the instrument during the first month of its on-orbit life, NICMOS is operating at a slightly higher temperature than was predicted (59.5 K instead of 57 K). The response of the

detector is temperature-dependent, so some changes are expected in the on-orbit flatfields relative to the thermal vacuum results. As part of the Cycle 7 calibration program, a full set of internal and external (earth) flatfields will be obtained. Users are encouraged to recalibrate their data with on-orbit flatfields if the pipeline calibration used thermal vacuum flatfields.

Preliminary results from SMOV indicate that variations in the large scale structure of the on-orbit flatfields relative to the thermal vacuum flatfields are of the order of 1–2% in Camera 2, and up to 5% in Camera 1. Figure 17.1 shows two examples of the ratio of the on-orbit to thermal vacuum flatfields for Camera 2 and Camera 1.

Figure 17.1: Ratio of On-Orbit to Thermal Vacuum Flatfields for Camera 2 in the F110W (left) and Camera 1 in the F140W (right). The ratios are averages across 20 columns and are given as a function of row number.

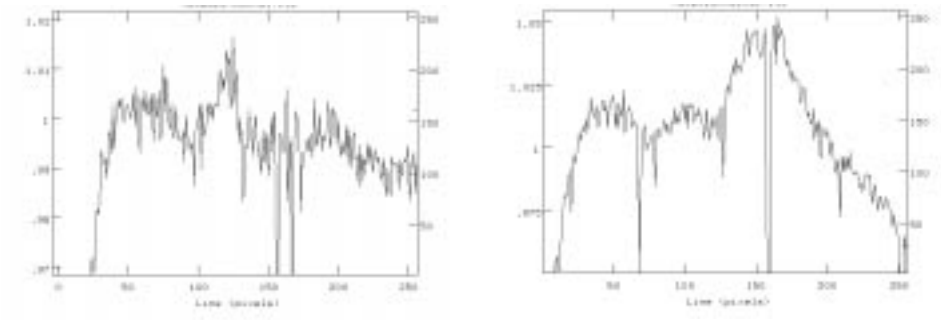

17.1.2 Characteristics and Uncertainties of Flatfields

Our current knowledge of the NICMOS flatfields is based on tests carried out using a flight spare detector array. The general characteristics are the same for the thermal vacuum flatfields, and we expect them to remain the same for on-orbit flatfields.

NICMOS flatfields show significant large-scale non-uniformity as well as pixel-to-pixel fluctuations. In addition, the non-uniformity is a strong function of the wavelength. Figure 17.3 shows the measured flatfield response for a flight spare array at a number of wavelengths. At 0.8 μm, the most sensitive areas on the array are more than twice as sensitive as the mean, and the least sensitive areas less than half as sensitive (i.e., there is variation by a factor of ~5 in the relative response across the array). This declines to a factor of ~3 at a wavelength of 2.2 μm, and at 2.5 μm the array is almost flat. We estimate that the mean uncertainties of the flat field response measurements are ~4%; the accuracy is however largely non-uniform, due to large variations in the response across the detector.

The amplitude of pixel-to-pixel variations in response is displayed in several ways in Figure 17.2, for a wavelength of 1.5 μm. The figure shows that the variations are essentially random with position on the array, and have a typical 1σ

amplitude ~8% and that the pixel-to-pixel variations are independent of the global response.

Figure 17.2: Flat Field Response Images Using 10% Bandwidth Filters on a Flight Spare Array. Wavelengths used include **(a)** 0.8μm, **(b)** 1.5μm, **(c)** 2.1μm and **(d)** 2.5μm. The images have been normalized to the mean response for each wavelength. The contours and greyscale are linearly spaced in each image between normalized responses of 0.4 and 2.2. Significant areas of the array span this whole range at 0.8μm, while at 2.5μm the array is almost flat.

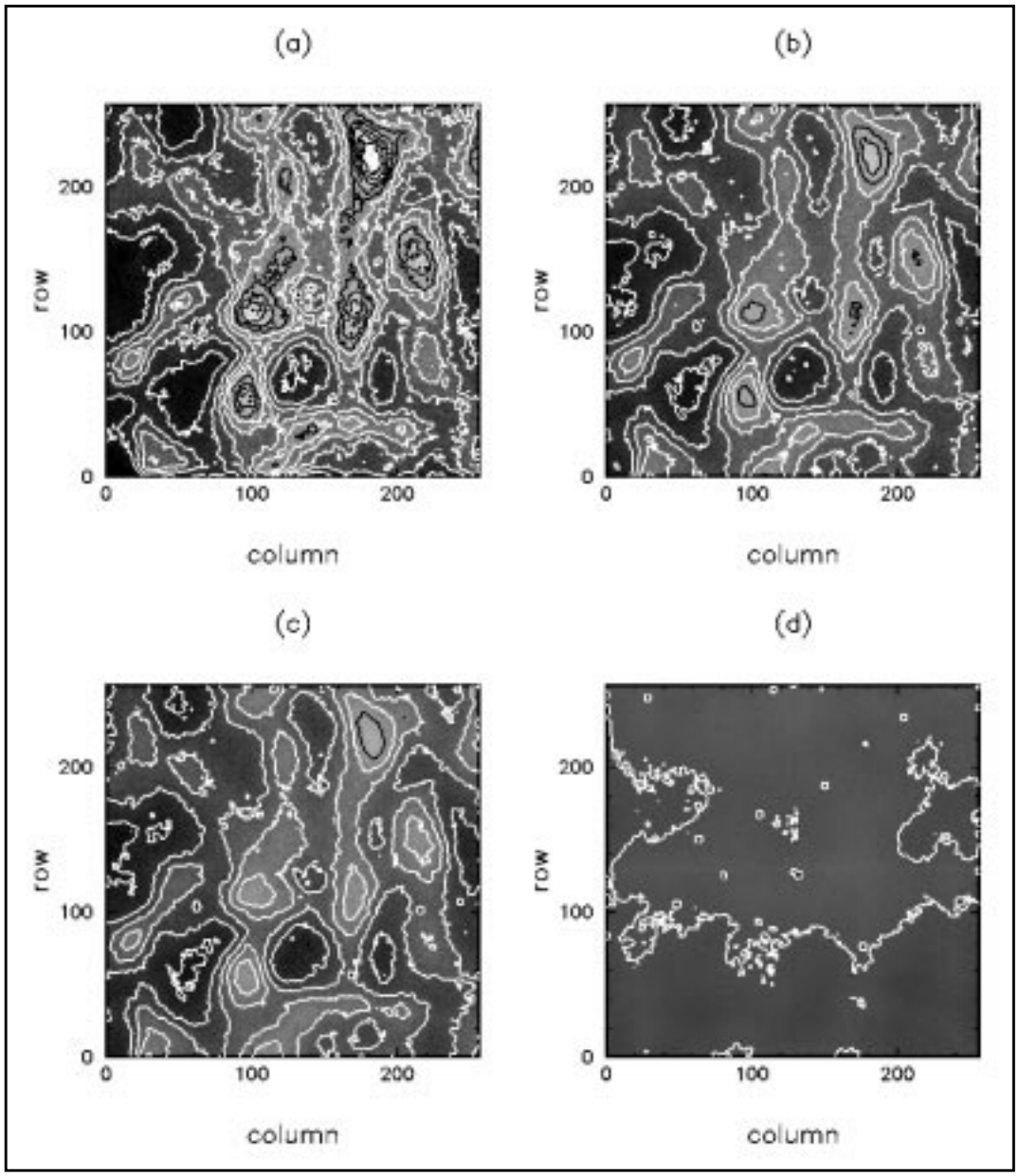

Figure 17.3: High Spatial Frequency Noise at 1.5µm. This was measured by dividing the image in Figure 17.2. (b) by a smoothed version of itself. The grey-scale version in **(a)** is scaled between 0.9 and 1.1. Slices through the image are plotted in **(b)** along row 100 and in **(c)** along column 100. The distribution of data is plotted as a histogram in **(d)**.

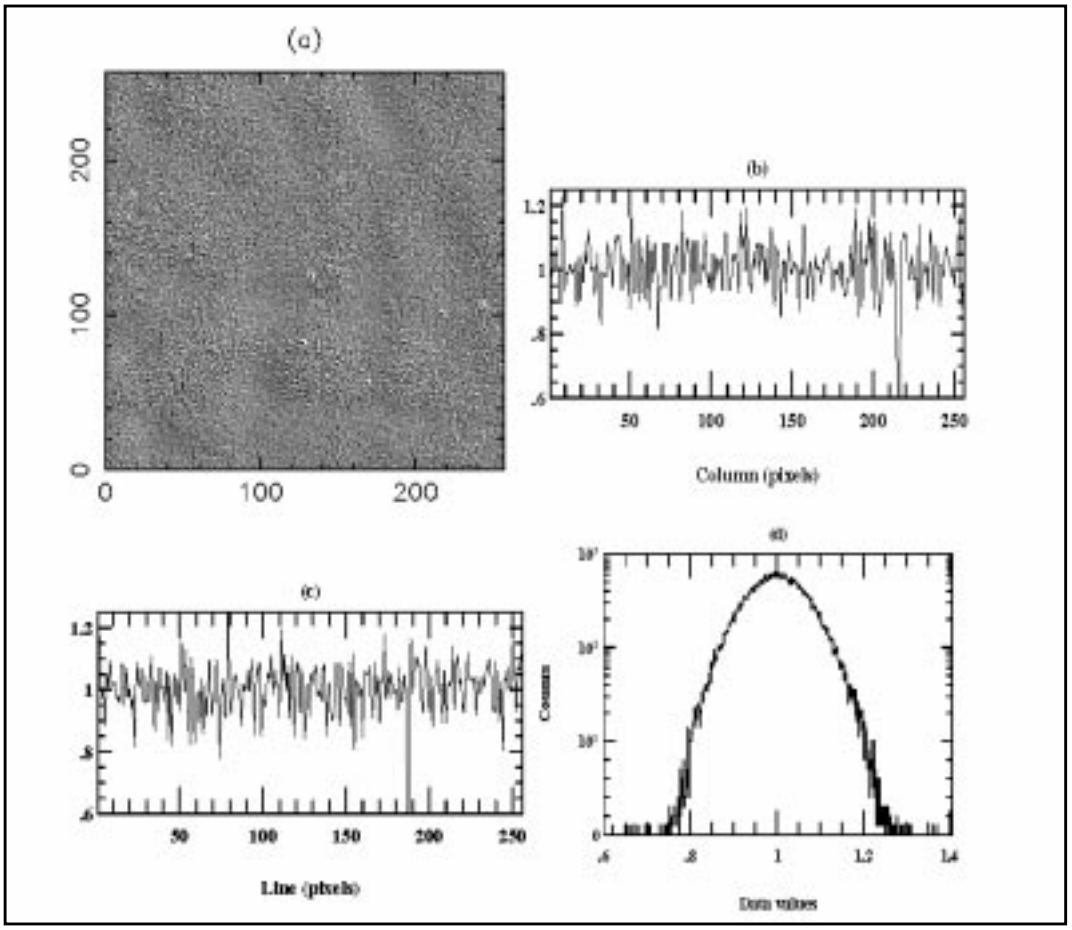

The size of the pixel-to-pixel sensitivity variations with wavelength is similar to that measured for spatial variations in the global flatfield response. At 0.8 µm the standard deviation of the pixel-to-pixel sensitivity variations is ~11%, at 1.5 µm it is ~7%, at 2.1 µm it is ~6%, and at 2.5 µm it is lower than the measurement uncertainties. Figure 17.4 shows the general behaviour of the flat-field response with wavelength, which is similar for low and high frequency variations.

The response of individual pixels relative to the mean of the array as a function of wavelength is given in Figure 17.5, for both low sensitivity and high sensitivity spots. The relative response is a slowly changing function of wavelength between 1.0 and 2.2 µm, while it changes dramatically beyond 2.25 µm, to become a linear function of wavelength.

In summary, NICMOS flatfields indicate:

- The flatfield response variations are large and wavelength dependent. The difference in response between the most and least sensitive areas is almost a factor of five at the shortest wavelengths and a factor of 1.1 at the longest wavelengths.
- The variation with wavelength is not linear, the largest variations occurring in small wavebands shortward of 1.1 microns and longward of 2.2 microns. The variations in response longward of about 2.2 microns are much more extreme than those shortward of 1.1 microns.
- The arrays exhibit wavelength dependent pixel-to-pixel response variations, ranging from an amplitude of order 10% at the shorter wavelengths to less than our measurement uncertainties at the longest wavelengths. The variation with wavelength of the pixel-to-pixel response variations is almost identical to the behavior of the global flat field response variations.

First indications from on-orbit flatfields are that all these characteristics are stable in time, and therefore calibratable with high accuracy. However, the change in temperature from the thermal vacuum experiments to the on-orbit operating conditions requires on-orbit flatfields to be used to calibrate NICMOS data.

Figure 17.4: Amplitude of Flat Field Response Variations as a Function of Wavelength. The solid line shows the global flat field response, defined as the standard deviation of the individual pixel responses, while the dashed line shows the pixel-to-pixel variations. The two follow the same behavior very closely.

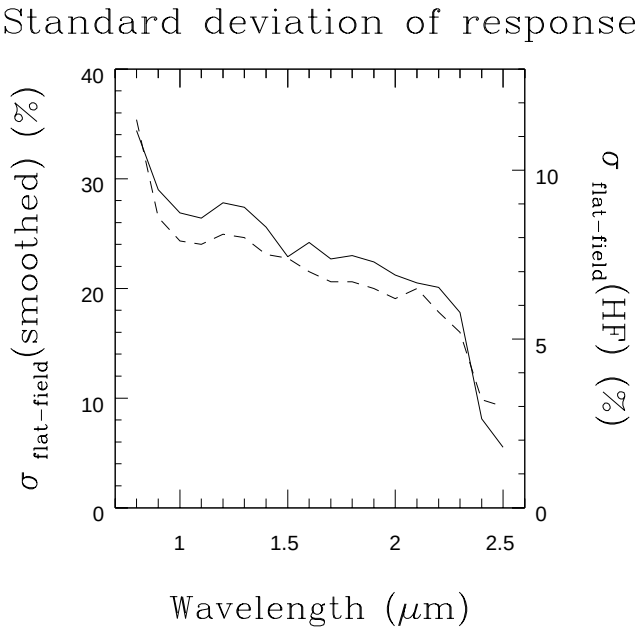

Figure 17.5: Responses of Selected Pixels Relative to the Mean of the Array as a Function of Wavelength. Both regions of low sensitivity (top panel) and high sensitivity (bottom panel) are considered. These figures show that the response flattens rapidly longward of 2.2 microns.

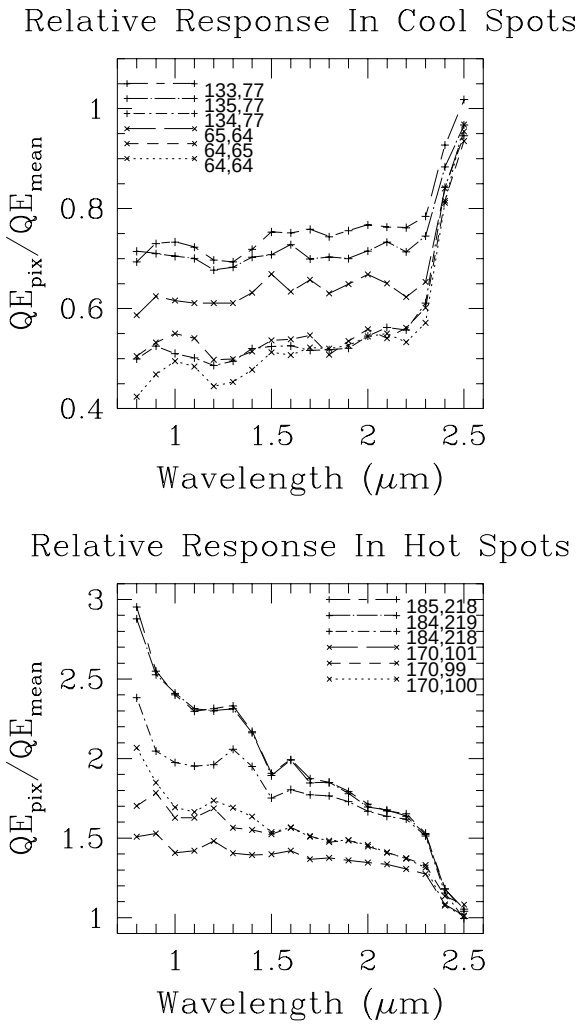

17.1.3 Color Dependence of Flatfields

The strong wavelength dependence of the NICMOS flatfields will affect the photometric accuracy of sources of extreme colors observed in broad-band filters. An estimate of the photometric accuracy which can be reached in these cases has been obtained simulating a source with color [J-K]=5 (equivalent to a blackbody with temperature T=700 K, e.g., a Young Stellar Object). The main result from the analysis is that the photometric errors are generally small: around 3% in the F110W and F140W filters, around 2% in the F205W filter, and less than 2% in the

other filters. However, they represent the limitation in photometric accuracy, unless multi-filter observations are available. In this case, an iterative correction procedure can be used to improve the photometric accuracy.

17.2 Dark Current Subtraction Errors

17.2.1 Dark Current Pedestal

NICMOS data show what is known as the *dark current pedestal*. This is an additive signal that appears whenever the detector's amplifiers are switched on, which happens at the beginning of an observing sequence, after a filter wheel motion, spacecraft motion, or Earth occultation. The level of the pedestal is quadrant-dependent and random, with typical values below 40–50 DN.

At the time of writing (August 1997) a flight software modification is being developed to remove the pedestal. The basic idea is to leave the amplifiers on at all times (instead of keeping them off, and switching them on only when exposures start). The degree to which this strategy has succeeded will not be known for some time after the change is made.

Being an additive signal, the most noticeable effect of the pedestal is to leave flatfield residuals in the calibrated images; the pedestal is a uniform offset without any flatfield variations, and so the flatfield correction step in **calnica** will impose an inverted flatfield response pattern in the final calibrated image. In addition, the absolute photometry of extended objects (i.e., those for which a reference sky level cannot be obtained within the frame) will be altered. Finally, the presence of the pedestal makes the **calnica** automatic cosmic ray rejection processing of MULTIACCUM images less effective. Since currently the pedestal effect lacks full characterization, it cannot be calibrated out by the pipeline.

For observations of compact sources, where most of the frame is occupied by blank sky, an iterative procedure can be used to remove most or all of the pedestal. The procedure exploits the large scale non-uniformity of the NICMOS flatfields, which will produce a large scale modulation of the blank sky in a calibrated NICMOS image with a considerable pedestal signal. The goal of the procedure is to remove the pedestal by minimizing the flatfield non-uniformities. This technique was thought out and developed by Mark Dickinson of the Johns Hopkins University, and is outlined below.

The procedure is iterative and identifies the minimum of the residual flatfield non-uniformities on the calibrated images (run through **calnica,** only). It should be applied on a quadrant-by-quadrant basis, becuase the pedestal level is different in different quadrants. For MULTIACCUM data, the procedure should be applied on individual imsets; however, it is not useful for the very first few readouts (where there is very little signal), and as a rule of thumb should be applied to those imsets with exposure times greater than about ten seconds. Increasing values of the pedestal level are subtracted from the each quadrant in the raw images, and the latter are run through the calibration software **calnica***, up to the flatfielding step*

only. The calibrated images are then smoothed (e.g., using the IRAF tool **rmedian**) to remove sources and pixel-to-pixel variations of the flatfield residuals. Finally, the variance of the residual large-scale modulation in each image is computed relative to the appropriate constant sky level. The pedestal level which yields the minimum for the variance is selected as the value for that particular quadrant. Because the reference value for the image is a constant sky level, it is clear why this technique can be applied only to those frames containing a large fraction of blank sky.

17.2.2 Synthetic MULTIACCUM Darks

NICMOS dark images are highly dependent on the readout history of the array since it was last reset, and, therefore, cannot be simply rescaled to the exposure time of the science data (as is done with most conventional CCD data). Each science file must be calibrated with a dark frame of equal exposure time and number of readouts.

A NICMOS dark frame can be decomposed into three basic components:

- Dark current proper.
- Amplifier glow.
- Shading (a bias change).

The three components are highly reproducible and can be easily calibrated. On-orbit darks obtained during SMOV have been used to characterize the dependence of the three components on the pixel position and on time for each of the three NICMOS detectors. This information has been used to construct synthetic dark current calibration reference files for all `MULTIACCUM` readout sequences, using as basic data the on-orbit darks obtained during the first part of the Cycle 7 calibration program. The synthetic darks have been used to populate the calibration database for those sequences for which on-orbit data do not exist yet or are currently contaminated by the dark current pedestal. These darks are routinely used to calibrate NICMOS data in the pipeline. Here we describe in more detail the three components of a synthetic dark.

Dark Current

The dark current component is the detector current when no external signal is present. This component is a function of time only:

$$D(t) = dc \times t$$

Where D is the observed signal in a given readout, t is time since reset, and dc is the dark current (e^-/s). The NICMOS dark current is of the order of 0.05–0.06 e^-/sec for Camera 2, and < 0.03 e^-/sec for Cameras 1 and 3.

Amplifier Glow

The characteristics of the amplifier glow are described in the section “Instrument Artifacts” on page 17-11. For the purpose of dark frame modelling, it is enough to know that the amplifier glow is a signal: infrared radiation emitted by

the amplifiers at the four corners of each NICMOS array, which is detected by the pixels in the array. It is like having a small light bulb in each corner, which produces a pattern of light that is highest in the corners and decreases towards the center of the array. Because the signal is injected in the array every time this is read, the amplifier glow depends on the number of readouts performed in a particular exposure. In particular, it is proportional to the number of readouts since the last reset:

$$A(x, y) = amp(x, y) \times NR$$

where *A(x,y)* is the cumulative signal due to the glow in a sequence, *amp(x,y)* is the amplifier glow signal per readout (a function of the pixel location *x,y*), and *NR* is the total number of readouts of the array since the last reset. In the corners of a full 26-readout MULTIACCUM response there will be of order 500–800 DN due to amplifier glow, as well as the associated Poisson noise from this signal. Because amplifier glow is a radiation source detected by the array, it is subject to the non-linearity and DQE characteristics of the array. The low-level non-linearity has not yet been well characterized, leaving some uncertainty in the correction. One standing problem for the characterization of the glow non-linearity is the unknown source signal in the science data images, since this is signal added to the amplifier glow signal and therefore contributes to the non-linear behavior. In many cases, the non-linearity is expected to induce small uncertainties in the final calibrated data.

Shading

Shading is a *noiseless* signal gradient, a pixel-dependent bias, orthogonal to the direction of primary clocking. The shading effectively changes the bias level for the pixels as a function of time and also of location, because the first pixels to be read show the largest bias change. Visually, this appears as a ripple and a signal gradient across a given quadrant of an uncorrected image. The amplitude of the shading can be as large as several hundred electrons for some pixels under some circumstances. The shading exhibits all the characteristics of a bias change, including lack of noise (within our measurement uncertainties). Through analysis of on-orbit dark data, we have determined that for a given pixel the bias level superimposed on the signal by the shading is dependent on the time since the last read (not reset) of the pixel. Thus if the time δt between reads remains constant, the bias level introduced by the shading remains constant. For MULTIACCUM readout sequences where the time between readouts is increasing logarithmically, the bias level changes with each successive read, and thus the overall shading pattern evolves with readout. The functional form of the shading is nearly exponential with δt and quite repeatable, although there are some circumstances when repeatability is not exact (namely, on orbit testing of the MIF sequences has shown that changing from a very long δt to a very short one introduces non-linearities in the functional form of the shading).

Although a numerical fit to the shading function is possible in principle, we have chosen to generate bias images for each of the δt of each of the

MULTIACCUM sequences from on-orbit data. In building a synthetic dark, the appropriate bias image:

$$B(x, y) = S(\delta t, x, y)$$

where *B(x,y)* is a function of the pixel location, can then be added to the other two components.

Making a Synthetic Dark

The total dark signal in *any given pixel* of any given NICMOS MULTIACCUM readout is just the sum of the three components above:

$$DARK(x, y, t) = D(t) + A(x, y) + B(x, y)$$

17.2.3 Uncertainties in the Synthetic Darks

The uncertainties in the dark frames described in this section are preliminary and will evolve as more on-orbit dark frames are obtained. Two types of uncertainties, random and systematic, can be identified in the synthetic darks.

Random Uncertainties

In the center of the NICMOS arrays, where the effects of shading and amplifier glow are smallest, the noise in the synthetic darks have uncertainties dominated by the readout noise. Because typically 15 measurements or so are used per read per pixel, the estimated uncertainities are of the order of 1 DN (about 5 electrons). In the corners of the arrays the amplifier glow is the largest source of noise, increasing as a function of the number of readouts. For the largest number of readouts (26) the estimated uncertainty is of the order of 5 DN (about 27 electrons). The random uncertainties in the dark frames are thus spatially dependent.

Systematic Uncertainties

Comparison of on-orbit to synthetic darks shows that the differences between the two are relatively small—on the order of 0 to 15 DN, with some excursions to 30–40 DN in the corners of the arrays for the final reads of full 26-readout sequences. Most of these differences are due to over- or under-subtraction of the amplifier glow. A better characterization of the amplifier glow from on-orbit data should alleviate these systematic effects.

The dark current pedestal adds some uncertainty to the synthetic darks, since on-orbit dark frames are used to generate synthetic darks. However, every effort was made to throw away pedestal-affected data when making the reference files currently in the database.

One standing problem is the proper shading correction in the second of the multiple readouts at the end of a MIF sequence. This single readout is the only one for which a shorter δt occurs after a longer one in any of the MULTIACCUM sequences. A different shading function is observed for this readout, lower by about 50–100 DN than expected for the specific δt, and with a smooth gradient

across a given quadrant in the readout direction. All previous and subsequent readouts appear unaffected by this problem. The effect of this one imperfect dark frame is typically rather small in the final calibrated image.

17.3 Instrument Artifacts

17.3.1 Non-Zero Zeroth Read Correction for Bright Sources

The first non-destructive read after a reset during a NICMOS exposure provides the reference bias level for the counts in each pixel of the science image. This is the zeroth read in a MULTIACCUM image, which is directly subtracted from the final readouts on-board the telescope for all the other readout modes so that only differences between non-destructive reads are sent back to the ground. Due to physical limitation in the readout speed, the zeroth read happens 0.203 seconds after the reset of the detector. When a bright source is being observed, a non negligible amount of charge will already have accumulated on the detector by the time the zeroth read is performed. (NICMOS doesn't have a shutter.) The consequences for the calibration of bright sources are obvious. Because the zeroth read subtraction from all subsequent readouts in a MULTIACCUM exposure is the first step of the calibration processing (and is automatically subtracted on-board the telescope from the final read in a ACCUM exposure), the handling of the detector nonlinear response will be inaccurate. At the time of this writing (August 1997) a modification of the calibration pipeline software **calnica** is being developed to correct the NICMOS observations for the non-zero zeroth read problem. The software fix requires that observations of bright sources be performed using the MULTIACCUM readout mode. The reason for this strategy is that all individual readouts are returned to the observer, and those can be used to extrapolate the counts back to the reset time (–0.203 seconds from the zeroth read) to recover the true bias level. Once the modification to the calibration pipeline software is in place, the problem will likely disappear. Then only the first few months of NICMOS on-orbit data taking will be affected (if bright sources have been observed), and those data may need recalibration.

17.3.2 Effects of Overexposure and the "Mr. Staypuft" Anomaly

Because each pixel of the NICMOS detectors is read individually, overexposure does not cause bleeding along the columns direction, unlike the case of CCDs. However, two artifacts result from the overexposure of one or more pixels:

- An afterimage with excess dark current persists for many minutes (>> 10). Decay of this signal depends both upon elapsed time and, fairly strongly, upon the number of readouts performed (ongoing modifications to the

autoflush procedure used between exposures may improve this situation). It is not unreasonable to expect signals of ~1 e^-/second up to an hour following a severe exposure.

- Extremely bright targets can result in faint phantom images at the same pixel locations in the other three quadrants of the detector. NICMOS arrays are divided into four quadrants of 128 x 128 pixels each. When a very large number of counts are recorded in a source at pixel (*i*,*j*) of any one quadrant, a faint ghost of this image appears at pixel (*i*,*j*) of each of the other three quadrants. A faint band is seen running along detector rows which pass through these ghosts, which could be mistaken for a diffraction spike. The amplitude of the ghost images is of order a tenth of a percent of the real image count rate. It appears to be an electronic phenomenon and is not an optical ghost. Inside the NICMOS group, this effect is known as the "Mr. Staypuft anomaly."

17.3.3 Vignetting

Lateral shifts of the dewar resulted in vignetting in all three cameras. In the case of NIC1 and NIC2, the source of the vignetting is most likely the Field Divider Assembly (FDA) mask. The losses in throughput are relatively small (< 5%) and affect only the first 30 rows of the arrays. In NIC3, the region affected by vignetting is larger than in the case of the other two cameras; the first 60 rows are vignetted. In this case, the source of vignetting is likely to be a combination of FDA and fore-optics. At the time of this writing (August 1997), we are evaluating the use of the Field Offset Mechanism (FOM) to move the aperture of NIC3, in order to correct at least the part of vignetting caused by the fore-optics.

17.3.4 Amplifier Glow

Each quadrant of a NICMOS detector has its own readout amplifier, which is situated close to an exterior corner of the detector. When a readout is made, the amplifier injects a real signal into the detector, known as *amplifier glow.* This signal is largest closest to the corners of the detector where the amplifiers are situated, and falls rapidly towards the center of the detector. The signal is only present during a readout, but is repeated for each readout (e.g., a MULTIACCUM sequence or an ACCUM with multiple initial and final reads). Typically the extra signal is about 20–30 DN at the corners of the detector and 2–3 DN at the center, for each readout. The signal is highly repeatable, and almost exactly linearly dependent on number of reads (however, there may be a small non-linearity for reads made very close together in time; the amplitude of this non-linearity typically amounts to only a fraction of DN accumulated over an entire `MULTIACCUM` exposure in the brightest parts of the amplifier glow signal, and our detection of this non-linearity is, at the time of this writing, marginal).

The amplifier glow is a real signal and is subject to photon statistics, so it is a source of noise in NICMOS exposures. Thanks to the repeatibility of the signal, images calibrated with the appropriate dark frames (same MULTIACCUM

sequence or same exposure time for ACCUM images) will have the amplifier glow removed. Its noise is propagated into the ERR array of the NICMOS calibrated images, thanks to its Poissonian nature.

17.3.5 Intra-Pixel Sensitivity Variations

As with many other modern array detectors, the sensitivity of the NICMOS detectors is lower near the edges of pixels then in their centers, causing reduced sensitivity along the intra-pixel boundaries. The response of a pixel to a source whose flux changes rapidly on a size scale comparable with or smaller than the pixel size will thus depend on where the center of the source lies with respect to the center of the pixel. Because the latter is not known a priori, this effect will introduce some uncertainty in the flux calibration for a point source. This uncertainty will be largest for Camera 3 at short wavelengths, for which the PSF is undersampled. We will try to measure the size of this effect on orbit and post updates on the NICMOS WWW pages; we expect it to be no more than a few percent uncertainty for Camera 3.

17.3.6 Hot Pixels, Cold Pixels, and Grot

The statistics on the cold and hot pixels present in each of the NICMOS cameras are presented in Table 17.1 below. In NIC2, the presence of the coronographic spot increases the number of cold pixels to 154.

In addition to these bad pixels which were already known from ground-based testing, more pixels have shown low measured quantum efficiency in orbit. These pixels are possibly affected by debris lying on top of the detectors. Paint flakes from the optical baffles are one possible source. Currently about 150–200 of these bad pixels have been measured in NIC1 and NIC2, and similar numbers are expected for NIC3. The bad pixels are often clustered in groups of up to 20–40, and appear as dark spots in flatfield frames. The position of the flakes varies.

Table 17.1: Statistics on Cold and Hot Pixels and Grot

Pixel Characteristic	NIC1	NIC2	NIC3
COLD	68	94	17
HOT	10	11	3
GROT	~ 200	~ 150	...

17.4 Cosmic Rays

As with CCDs, cosmic ray hits will produce unwanted signal in the output images, but hot pixels are not expected to develop from such hits. Hence, cosmic rays should have little impact on the long-term array performance in orbit.

Analysis of SMOV data has shown that the rate of cosmic rays on the NICMOS detectors is about 1.2–1.6 events/Camera/sec (5 σ detections, see *Instrument Science Report* NIMOS-022). The mean size of the cosmic ray (CR) hits is 1.65 to 2 pixels. Table 17.2 below summarizes cosmic ray statistics for the three cameras, for 5 σ and 3 σ detections. The numbers for Camera 2 come from two different programs and indicate variations of about 60% in the rate of CR-affected pixels between the two observations; the variations reflect changes in the orbital position of the telescope relative to the South Atlantic Anomaly. This level of variation is what should be expected during a typical multi-orbit program.

Table 17.2: CR Event Statistics

Camera	Threshold	Affected Pixels (#/Camera/sec)
NIC1	5 σ	2.11
NIC1	3 σ	2.74
NIC2	5 σ	1.99-3.21
NIC2	3 σ	2.43-3.96
NIC3	5 σ	1.90
NIC3	3 σ	2.79

For a mean CR-affected pixel rate of about 2.5 pixels/sec, about 8% of the pixels in the detector will show cosmic ray events in a 2000 second exposure.

CR hits should be detected by **calnica** in MULTIACCUM data, and will be flagged in the DQ extensions of the `*_ima.fits` files.

17.5 Calibration Goals

The Cycle 7 calibration goals for NICMOS are listed in Table 17.1 below. Since NICMOS is expected to run out of cryogens between the end of 1998 and the beginning of 1999, these represent the final calibration goals for the instrument. The main limiting factor for attaining such goals will be the thermal stability of the instrument. The Table summarizes the accuracy we expect to

achieve for reference files, photometry, astrometry, etc. (see the *NICMOS Instrument Handbook*).

Table 17.1: NICMOS Calibration Goals

Attribute	Accuracy	Comments/Limiting Factors
MULTIACCUM and ACCUM darks	10 ADU	All three detectors. All the supported MULTIACCUM sequences and a subset of ACCUM exposure times will be calibrated to this accuracy. Other ACCUM exposure times will require interpolation.
Flatfields	2% global uncertainty <1% pixel-to-pixel	NIC1 and NIC2 (reduced program for NIC3). Flatfields will be obtained from a combination of internal lamp flats (1% accuracy, polarizers, broad and medium band filters) and Earth flats (2% acccuracy, narrow band filters). Color dependence may limit flatfields in some cases.
Photometry	5-10% absolute 2% relative over field-of-view 2% stability	Main limiting factors: accuracy of standards; filter leaks on red sources
Focus position	maintained within 1 mm	Instrument focus will be monitored throughout the entire Cycle 7 in all three cameras
Polarizers	1% relative photometry 3–5% absolute polarization	Instrumental polarization and zero position angle of NIC1 and NIC2 will be measured. Limiting factors: dark and flatfield uncertainties; polarizing efficiency.
Grisms	0.01 μm (wavelength calibration) 20%-30% (absolute and relative photometric sensitivity)	Expected accuracy over central 80% of spectral range. Grism C flat may not achieve the declared accuracy.
Coronagraph	0.019" positioning	Hole and detector are not at common focus
NICMOS to FGS astrometry	0.1"	
Plate Scale Calibration	0.2%	

Chapter 18
NICMOS Data Analysis

In This Chapter...

This chapter describes specific tools and topics related to the analysis of the NICMOS data. The first section points out some STSDAS tools for analyzing NICMOS images. The remainder of the chapter deals with topics of more or less general interest: photometric calibration, PSF subtraction, and polarimetric analysis.

18.1 STSDAS Software

Software tools for NICMOS FITS files now available in the STSDAS packages **toolbox.imgtools.mstools** and **hst_calib.nicmos** have been designed to maintain compatibility with pre-existing analysis software. The tools have either been written in ANSI-C or are IRAF CL scripts interfacing with pre-existing IRAF/STSDAS tasks. Some of the new tools will accept a variety of data formats such as OIF and GEIS, as well as STIS and NICMOS FITS files, and will in time replace the STSDAS tasks they render obsolete.

The new tasks fall into two major categories:

1. ***General-purpose utilities***. These tasks include tools for mathematical and statistical operations on science images and for analysis and display of reduced and raw data. In most cases, the new utilities extend existing routines to include error and data quality propagation. These are the utilities of greatest interest to the user community. Under this category are several

tasks described in Chapter 3, **msarith**, **mscombine**, **msstatistics**, **msjoin** and **mssplit**, along with a few other tasks we describe below, **ndisplay**, **markdq**, and **pstack**. The first five are found in the package **toolbox.imgtools.mstools**, the remaining ones reside in the package **hst_calib.nicmos**.

2. ***Calibration-oriented utilities***. These tasks generate reference files, such as readnoise arrays, dark files, flatfields, non-linearity correction arrays, and bad pixel arrays, to feed the calibration database and to support the calibration pipelines. The tasks are designed specifically for the calibration of NICMOS and will not be of general utility. The tools are **mstreakflat**, **msbadpix**, **ndark**, **nlincorr**, and **msreadnoise**. All are located in the calibration package **hst_calib.nicmos**.

The tasks in the **toolbox.imgtools.mstools** package are particularly useful for working with individual STIS and NICMOS imsets. See “Working with STIS and NICMOS Imsets” on page 3-12 if you are not familiar with these tasks. Below we describe a few tasks of specific interest to NICMOS observers. For additional details and examples of these and other tools, please refer to the online help.

ndisplay and markdq

The **markdq** task reads the data quality (DQ) array from a NICMOS image and marks the DQ flags on the displayed image. Each flag value can be set independently to a different color or can be turned off. The **ndisplay** task combines the capabilities of the IRAF task **display** and the task **markdq**: it displays a NICMOS image and overlays the DQ flags according to a user-specified color-code. Both tasks are useful for locating specific DQ values, for example, the cosmic rays rejected by **calnica** in a MULTIACCUM image.

pstack

The **pstack** task plots all the samples of the specified pixels from a NICMOS MULTIACCUM image as a function of time. This task can be used to track the time behavior of an image on a pixel-by-pixel basis. For example, the temporal positions of cosmic ray hits or the onset of saturation during the course of an exposure can be located for a defined set of pixels.

18.2 Photometric Calibrations

Being above the atmosphere, NICMOS is not forced to adopt filter bandpasses like instruments used at ground-based observatories, but instead it has filters constrained by anticipated scientific demands. Thus in practice NICMOS does not have filters matched to any of the ground-based photometric bands. Obtaining photometric calibrations for NICMOS data is discussed in this section; cases of continuum sources, emission lines, and grism spectra will be presented.

18.2.1 Units for NICMOS Photometry

Given the multitude of units and systems that have been used for infrared (IR) photometry (magnitudes, Jy, W m^{-2} μm^{-1}, erg sec^{-1} cm^{-2} μm^{-1}, etc.) and given the lack of a standard for ground-based IR filters, NICMOS has adopted the IRAS approach, where the calibrated data were presented in Janskys (Jy), or Jy $arcsec^{-2}$ for surface brightness data. Details on how to transform different sets of units can be found in Chapter 12 of the *NICMOS Instrument Handbook* or obtained using the Unit Conversion Program in the NICMOS WWW software tools page.

18.2.2 Fluxes and Magnitude Zeropoints

The NICMOS calibration pipeline provides two photometric parameters for the conversion of countrates into fluxes. These parameters are found in the keywords PHOTFNU and PHOTFLAM in the header of the calibrated image. PHOTFNU is given in units of Jy sec DN^{-1} and PHOTFLAM in units of ergs cm^{-2} $Å^{-1}$ DN^{-1}. Because NICMOS calibrated data are given in countrate, i.e., DN sec^{-1}, the countrate to flux conversion is simply achieved by multiplying the countrate by the PHOTFNU or PHOTFLAM value, depending on which units are desired for the final calibrated image.

A list of current PHOTFNU and PHOTFLAM values for all available filters are given in Table 18.1 through Table 18.3. These values are the result of the on-orbit SMOV photometric characterization and are preliminary. The SMOV photometric characterization used a small subset of filters for each of the cameras; a full calibration of NICMOS photometric performance as a function of wavelength is not available yet. Our best estimates indicate that the values listed in the tables have uncertainties at the 10–15% level, on average. A complete characterization of NICMOS photometric performance will be obtained as part of the Cycle 7 calibration program and the PHOTFNU and PHOTFLAM values will then be updated. The revised photometric table will then be posted on the NICMOS WWW pages.

In the header of your calibrated images, there are three additional photometric parameters that characterize the filter used for the observation (PHOTPLAM and PHOTBW) and provide the ST magnitude zero point (PHOTZPT). PHOTPLAM gives the value of the pivot wavelength of the filter in Angstroms. This wavelength is source-independent and is the wavelength for which:

$$PHOTFLAM = c \times PHOTFNU \times PHOTPLAM^{-2}$$

where *c* is the speed of light in vacuum. PHOTBW gives the rms band of the filter in Angstroms (see the *Synphot User's Guide* for a detailed definition of both parameters).

The magnitude of an object can be determined in the ST system (e.g., based on a constant flux per unit wavelength) using the photometric zero-point keyword PHOTZPT (= -21.1) simply by:

$$m_{ST} = -2.5\log(PHOTFLAM \times CR) + PHOTZPT$$

$$= -2.5\log(PHOTFLAM \times CR) - 21.1$$

where *CR* is the count rate in units of DN sec^{-1}. On the other hand, the magnitude in Oke's AB_ν system (e.g., based on a constant flux per unit frequency) is obtained by applying the following expression:

$$m_{AB} = -2.5\log(10^{-23} \times PHOTFNU \times CR) - 48.6$$

$$= -2.5\log(PHOTFNU \times CR) + 8.9$$

Zeropoints for magnitudes based on the Vega system are reported in the last column of Table 18.1 through Table 18.3 in units of Jy. The zeropoints for the NICMOS bandpasses are derived from the reference spectrum of Vega generated at the STScI (Colina, Bohlin & Castelli 1996, ISR CAL/SCS-008), assuming Vega has a magnitude equal to 0.02 in all NICMOS bandpasses, as per the calibration of Campins et al. (1985, *AJ*, 90, 896). The reference spectrum has been multiplied by a factor 1.05 to correct for the 5% discrepancy between the model and the near infrared measurements. The conversion from count rates to magnitudes in the Vega system is given by the standard formula:

$$m = -2.5\log(PHOTFNU \times CR \times ZP(Vega)^{-1})$$

Details about plans to define an HST JHK system and compute the photometric transformations to ground-based systems are given in "Magnitudes and Photometric Systems Transformations" on page 18-8.

18.2.3 Photometric Corrections

Differential Photometry

The photometric values provided in the headers are obtained from measurements of standard stars in the central regions of the detectors. Both high frequency (pixel-to-pixel) and low frequency (large-scale structures) sensitivity variations will be corrected using on-orbit flats. Preliminary SMOV differential photometry characterization of NICMOS cameras indicate that residual large scale deviations could amount to ~2%, except in the corners that might be higher. A Cycle 7 calibration program has been designed to measure with a fine grid the photometric deviations from the average as a function of wavelength, for each camera. A correction image might be generated as a product of this program, if measurable deviations are found.

Table 18.1: NIC1 Photometry

Spectral Element	PHOTFLAM (erg cm^{-2} A^{-1} DN^{-1})	PHOTNU (Jy sec DN^{-1})	ZP(Vega) (Jy)
F090M	5.349E-18	1.459E-5	2305.9
F095N	7.634E-17	2.316E-4	1854.1
F097N	6.163E-17	1.941E-4	2372.0
F108N	3.614E-17	1.411E-4	2011.8
F110M	1.739E-18	7.051E-6	1947.2
F110W	6.379E-19	2.713E-6	1897.0
F113N	2.922E-17	1.244E-4	1890.9
F140W	2.253E-19	1.558E-6	1395.4
F145M	9.020E-19	6.376E-6	1278.9
F160W	3.266E-19	2.814E-6	1111.6
F164N	7.323E-18	6.618E-5	1018
F165M	6.120E-19	5.551E-6	1032.5
F166N	6.975E-18	6.416E-5	1080.1
F170M	5.306E-19	5.156E-6	1011.1
F187N	5.051E-18	5.922E-5	826.6
F190N	4.842E-18	5.822E-5	861.5
POL0S	1.171E-18	4.392E-6	2027.9
POL120S	1.171E-18	4.392E-6	2027.9
POL240S	1.171E-18	4.392E-6	2027.9

Pixel Centering

As with many other array detectors, the sensitivity of the NICMOS detectors is lower near the edges of the pixels than in their centers. It is as though there were small regions of reduced sensitivity along the intra-pixel boundaries. In practical terms this effect means that for a source whose flux changes rapidly on a size comparable with or smaller than the pixel size, the measured countrate, and therefore flux, will depend on where the center of the source lies with respect to the center of the pixel. Because this position is not known a priori, this effect will introduce some uncertainty in the flux calibration for a point source. This uncertainty will be largest (no more than a few percent, we expect) for NIC3 at short wavelengths, in which the PSF is undersampled. For high precision photometry and to compute the amount of photometric uncertainty in a particular camera and filter combination due to this effect, subpixel dithering is recommended.

Table 18.2: NIC2 Photometry

Spectral Element	PHOTFLAM (erg cm-2 A-1 DN-1)	PHOTNU (Jy sec DN^{-1})	ZP(Vega) (Jy)
F110W	5.626E-19	2.390E-6	1898.3
F160W	2.939E-19	2.529E-6	1113.0
F165M	5.484E-19	4.990E-6	1051.1
F171M	1.232E-18	1.217E-5	995.4
F180M	1.185E-18	1.277E-5	931.5
F187N	4.336E-18	5.079E-5	828.2
F187W	3.858E-19	4.509E-6	873.1
F190N	4.293E-18	5.171E-5	860.6
F204M	5.946E-19	8.217E-6	766.0
F205W	9.167E-20	1.312E-6	752.5
F207M	3.787E-19	5.478E-6	734.6
F212N	2.325E-18	3.490E-5	710.9
F215N	2.493E-18	3.840E-5	690.0
F216N	2.236E-18	3.494E-5	648.1
F222M	3.099E-19	5.086E-6	652.9
F237M	2.329E-19	4.363E-6	584.0
POL0L	3.164E-19	4.225E-6	785.1
POL120L	3.164E-19	4.225E-6	785.1
POL240L	3.164E-19	4.225E-6	785.1

PSF Variations

The point spread function (PSF) of the telescope changes with time, and these changes will affect photometry using very small (less than 3-4 pixel radius) apertures. Changes in focus observed on an orbital timescale are due mainly to thermal breathing of the telescope. In addition to this short term PSF variation there is an additional long-term NICMOS component, as the cryogen evaporates and the dewar relaxes. As a result of the stress produced by the solid nitrogen on the instrument, NICMOS detectors have been moving, and keep moving, along the focus direction. The motion of the cameras is monitored twice a month and NICMOS focus updates can be periodically implemented, if required. Although preliminary results from SMOV indicate that the breathing effects on small aperture photometry are below our measurement precision (a few percent), the subject is still under investigation.

Table 18.3: NIC3 Photometry

Spectral Element	PHOTFLAM (erg cm-2 A-1 DN-1)	PHOTNU (Jy sec DN^{-1})	ZP(Vega) (Jy)
F108N	4.335E-17	1.687E-4	2021.2
F110W	6.794E-19	2.875E-6	1903.9
F113N	3.315E-17	1.408E-4	1894.8
F150W	2.008E-19	1.606E-6	1238.2
F160W	3.462E-19	2.985E-6	1111.1
F164N	7.738E-18	6.993E-5	1032.5
F166N	7.778E-18	7.135E-5	1081.5
F175W	9.150E-20	1.029E-6	971.5
F187N	5.220E-18	6.120E-5	826.6
F190N	4.994E-18	6.015E-5	860.6
F196N	4.227E-18	5.438E-5	809.9
F200N	3.810E-18	5.070E-5	791.1
F212N	2.675E-18	4.016E-5	710.9
F215N	2.854E-18	4.396E-5	689.9
F222M	3.519E-19	5.777E-6	652.8
F240M	2.017E-19	3.865E-6	571.7
G096	1.641E-18	5.560E-6	2138.9
G141	2.614E-19	2.102E-6	1235.5
G206	8.583E-20	1.178E-6	817.9

Aperture Correction

It is often difficult to measure the total flux of a point source due to the extended wings of the PSF, difraction spikes, and scattered light. Such measurements are particularly difficult in crowded fields where the extended wings of well resolved sources can overlap with each other. An accurate method of measuring the integrated flux in these situations could consist of several steps:

1. Measure in the image the total counts within a small radius.
2. Simulate the TinyTim[1] PSF for the particular camera-filter combination and position in the detector.
3. Measure in the simulated PSF image the fraction of total flux within the selected aperture.

1. TinyTim software can be retrieved from the Web at: `http://scivax.stsci.edu/~krist/tinytim.html`

To obtain the total flux of the source, the countrate then only needs to be multiplied by the PHOTFNU or PHOTFLAM value and by the inverse of the measured fraction obtained in step three above.

Empirical PSFs could also be used for the above mentioned method. However, there are no plans to obtain PSF profiles for all camera and filter combinations as part of the Cycle 7 calibration plan. Empirical PSFs for the central regions of the detectors can be obtained from the calibrated images obtained for the Cycle 7 absolute photometry (proposal 7691) and photometric monitoring (proposal 7607) programs.

Red Leaks

Many very red targets will be observed with NICMOS at short wavelengths (~1 μm). For these sources the flux at ~2.2–2.5 μm could be orders of magnitude larger than at ~1.0 μm and therefore exceptionally good out-of-band blocking would be required. Pre-launch tests indicated that for very red sources (temperature ~700 K and lower), the photometric errors induced by red leaks might be as large as an order of magnitude in a few filters. The filters for which red leaks might be a problem are: F090M, F095N, F097N, F108N, F110M, F110W, F113N, F187N and F190N. Strategies involving observations in multiple filters to model the source spectral energy distribution are required in these cases. Observations of a very red star will be obtained as part of the Cycle 7 calibration plan and the results will be posted on the Web.

Non-Zero Zeroth Read Correction for Bright Sources

The problem of the non-zero zeroth read for bright sources was discussed in Chapter 17. If a non-zero zeroth read is present, corrections for the detector's non linear response may not have been taken into proper account by the current version of the pipeline (as of August 1997). It is advisable to reprocess the data with the most recent version of the calibration software (at the time of this writing, early August 1997, the software modification for **calnica** that should remove the problem in the pipeline is under testing; data processed after the new software is installed in the pipeline should be free of the non-zero zero read problem).

18.2.4 Magnitudes and Photometric Systems Transformations

As previously mentioned, NICMOS data will be calibrated in units of Jy or Jy arcsec^{-2}. There are currently no plans to compute color corrections and to provide transformations to convert HST fluxes into ground-based magnitude systems. However, as part of the Cycle 7 absolute photometry program, we will observe a few blue stars (white dwarfs), intermediate color stars (solar analogs), and very red stars covering a large range in color (Table 18.4). The calibrated data will be made available immediately for users requiring to transform their HST fluxes into any ground-based system. The recommended HST JHK-analog system is obtained using the F110W, F160W and F222M filters.

Table 18.4: List of Stars for Photometric Transformations

Name	H	J-H	H-K	Status
G191-B2B	12.6	-0.10	-0.14	Primary standard (white dwarf).
P330E	11.6	0.28	0.07	Primary standard (solar analog).
OPH-S1	7.3	1.53	0.94	Primary standard (red standard).
GD71	13.8	-0.08	-0.13	Pending approval (white dwarf).
P177D	12.0	0.28	0.06	Pending approval (solar analog).
CSKE_12	9.5	2.08	0.89	Pending approval (red standard).
BRI0021	11.1	0.75	0.52	Pending approval (red standard).

18.2.5 Absolute Photometry for Emission Line Filters

The narrow band filters in NICMOS are intended primarily for observations of emission or absorption lines in sources. Because the photometric conversion factors PHOTFNU and PHOTFLAM for all NICMOS filters are obtained from continuum observations of emission-line free standard stars, the flux in erg sec^{-1} cm^{-2} of an emission line is given by the expression:

$$Flux_{line} = 1.054 \times FWHM \times PHOTFLAM \times CR$$

where FWHM is the full width half maximum of the equivalent gaussian filter to the narrow-band filter used (see Chapter 11 of the *NICMOS Instrument Handbook*), and we have assumed that the continuum has been already subtracted from the total flux in the filter and that the line is centered in the filter. If the emission line is not at the central wavelength of the filter, the line flux will need correction for the filter transmission curve. To estimate the variation in the absolute flux due to the positioning and width of the emission line in the filter bandpass, the **synphot** task **calcphot** can be used as shown below. See the *Synphot User's Guide* for additional help.

Figure 18.1: Estimating Absolute Flux Variation

```
sy> epar calcphot
obsmode = nicmos,3,f212n,dn Instrument observation mode
spectrum= gauss(21200,40)*unit(1E-13,flam) Synthetic spectrum to calculate
form = counts Form for output data
(func = effstim) Function of output data
(vzero = ) List of values for variable zero
(output = none) Output table name
(append = no) Append to existing table?
(wavetab= ) Wavelength table name
(result = 0.) Result of synphot calculation for form
(refdata= ) Reference data
(mode = a)

sy> epar calcphot
obsmode = nicmos,3,f212n,dn Instrument observation mode
spectrum= gauss(21280,40)*unit(1E-13,flam) Synthetic spectrum to calculate
form = counts Form for output data
(func = effstim) Function of output data
(vzero = ) List of values for variable zero
(output = none) Output table name
(append = no) Append to existing table?
(wavetab= ) Wavelength table name
(result = 0.) Result of synphot calculation for form
(refdata= ) Reference data
(mode = a)
```


The examples above compute the countrate in the NIC3 F212N filter for a H_2 (2.12 micron) emission line having a gaussian profile of 40 Angstroms and a peak flux of 1.0 x 10^{-13} erg sec^{-1} cm^{-2} A^{-1}. The integrated flux will then be 4.2 x 10^{-12} erg sec^{-1} cm^{-2}. In the first example the H_2 emission line is at zero redshift and centered on the filter while in the second example the line is redshifted by 80 Angstroms. If the emission line is centered on the filter, the H_2 flux will produce 7421.1 DN sec^{-1} while the countrate will be ~90% of this value (i.e., 6662.3 DN sec^{-1}) for the redshifted emission line. The expression for the $Flux_{line}$ above can be directly applied to the first case, while a correction factor 1.11=(7421.1/6662.2) is needed in the second case.

18.2.6 Absolute Spectrophotometry with NICMOS Grisms

The accuracy of the absolute spectrophotometry with NICMOS grisms depends on three different limiting factors:

- Accuracy of the spectral energy distribution of the standard stars used to obtain the inverse sensitivity curve.
- Quality of the flat-fielding and background subtraction of the calibration observations.
- Quality of the flat-fielding and background subtraction of the science observation itself.

The major source of uncertainty in the absolute spectrophotometry of a given source comes from the variability and structure of the background. Every pixel on the NIC3 array will receive background radiation over the entire spectral bandpass of the particular grism, while the source spectrum will be dispersed. The accuracy of the background subtraction is limited by our knowledge of the spectral response of each pixel, which is somewhat different from pixel to pixel. Extracted

spectra will have to be corrected for the spectral response of each pixel. The accuracy of this correction is again limited by our knowledge of the detector response.

The absolute flux calibration of the spectral energy distribution of the standard stars in the 0.8 to 2.5 μm wavelength range is known to 2–5%. Characterization of the grisms' absolute sensitivity during SMOV indicates that the absolute calibration of grism spectrophotometry for bright sources, i.e. well above background, will have a total 20–30% uncertainty. For Grism C the uncertainties could be even higher because of the large thermal background in this wavelength range (1.4 to 2.5 μm).

18.3 PSF Subtraction

Accurate PSF subtraction is a prime concern for an observer wishing to study faint features around bright objects. Typical situations are: host galaxy harboring a bright quasar; circumstellar nebulosity around a bright star; faint companions of a bright star, etc. The PSF subtraction technique has proved to be very successful in this kind of studies for HST data obtained with WFPC2. But imaging with NICMOS cameras 1 and 2 can probably easily exceed the success of WFPC2 thanks to a few important advantages:

- Cameras 1 and 2 provide images which are diffraction limited, well sampled, and better resolved (see Figure 18.1 and Figure 18.2).
- The MULTIACCUM mode automatically provides sub-exposures at different times as a way to look at increasingly faint features at different distances from the bright central source.
- For saturated bright central point source, there is no blooming along the detector array columns.

The best way to get a high quality PSF for PSF subtraction is to measure an isolated bright unsaturated star in the same image or to construct a composite PSF using good stars in the image. This can be accomplished using the IRAF **digiphot** package as described in *A User's Guide to Stellar CCD photometry with IRAF*[2]. A PSF obtained from the same image, along with a number of obvious advantages, also takes care of the *breathing* effect (variations of focus position due to thermally induced mechanical displacements in the HST optical path). If no suitable star can be found in the image, one can resort to a synthetic PSF computed using TinyTim.

2. This and other relevant IRAF documents can be obtained from the IRAF Web site at: `http://iraf.noao.edu/`.

Figure 18.2: NIC1 Image with PSF Radial Profile

Image of Star Taken with NIC1 F165M **PSF Radial Profile**

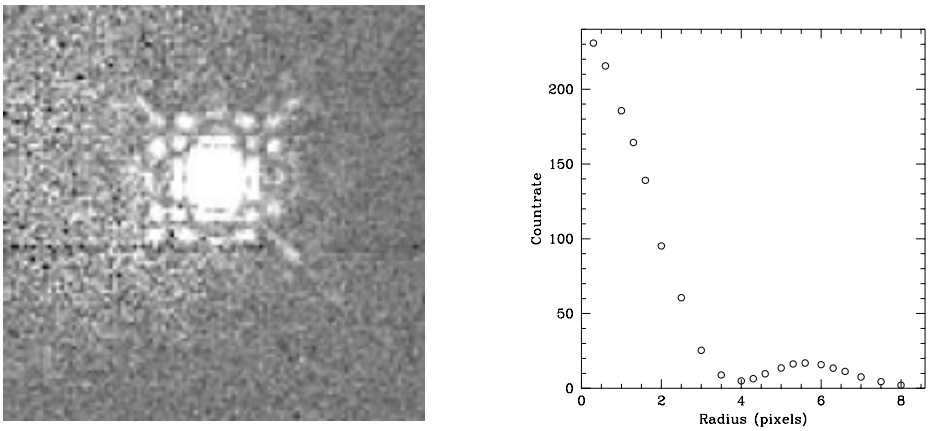

Figure 18.3: NIC2 Image with Radial Profile

Image of Star Taken with NIC2 F237M **PSF Radial Profile**

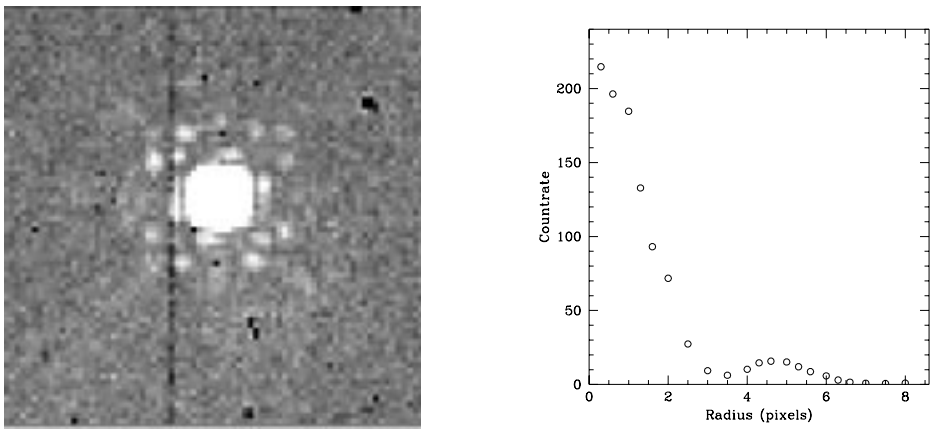

18.4 Analysis of Polarization Images

18.4.1 Introduction

The analysis of NICMOS polarization images is aimed at determining the Stokes' Parameters, and from those the polarization angle and degree for each pixel. NICMOS Camera 1 and Camera 2 each contain three polarizers, whose principal axes of transmission are separated by 120 degrees. The spectral coverage is fixed for each Camera, with wavelength coverage 0.8–1.3 μm in Camera 1 and 1.9–2.1 μm in Camera 2. A complete set of polarimetric observations will contain images obtained in all three polarizers of the selected wavelength range. We assume that each image has been processed through **calnica** and **calnicb** to produce a fully reduced and (if necessary) mosaiced image in each of the three

filters, with the data corrected for saturation and cosmic rays and converted to flux density.

The images in the three filters need to be compared, in order to produce the Stokes' parameters. To do so, the three images need to have the same dimensions and to be registered (have the source centered at exactly the same location in each image). In principle they should already be registered, provided the images in each filter were taken in the same visit without any changes of guide stars. If there is any displacement of the source between images, then each image can be registered using the IRAF task **imlintran**. When **imlintran** is used, the origin for the three input images should be set to the location of the source in each, so that in the output images the origin and the parameters *nlines* and *ncolumns* are identical.

To generate Stokes' parameters, the relative differences in flux between images in the different polarizing filters are used. Where the signal level is very faint, and the signal-to-noise ratio is very low, the differences will be very large but dominated by noise. If you attempt to calculate the Stokes' parameters using such data, you will obtain large and entirely spurious polarizations. To avoid this problem, it is advisable to estimate the noise in an area of the image free of sources, and then set a threshold at a value of order five to ten times this noise level. Using the IRAF task **imreplace**, all pixels with signals below this threshold should be set to some arbitrary value, probably close to the measured noise level. This action will cause all areas of the image where the signal level is very faint to show zero polarization.

18.4.2 Theory

If we define the intensity and statistical uncertainties (including read-noise) obtained in the three polarizers to be I_0, I_{120} and I_{240} and σ_0, σ_{120}, σ_{240} respectively, then we may obtain the total intensity *I* from:

$$I = \frac{2}{3}(I_0 + I_{120} + I_{240})$$

and the Stokes parameters Q and U:

$$Q = \frac{2}{3}(2I_0 - I_{240} - I_{120})$$

$$U = \frac{2}{\sqrt{3}}(I_{240} - I_{120})$$

The statistical uncertainties are obtained by straightforward propagation of errors:

$$\sigma_I = \frac{2}{3}\sqrt{[\sigma_0^2 + \sigma_{240}^2 + \sigma_{120}^2]}$$

$$\sigma_U = \frac{2}{\sqrt{3}}\sqrt{[\sigma_{240}^2 + \sigma_{120}^2]}$$

$$\sigma_Q = \frac{2}{3}\sqrt{[4\sigma_0^2 + \sigma_{240}^2 + \sigma_{120}^2]}$$

The Stokes parameters can then be combined to yield the polarized intensity, $I_{p:}$

$$I_p = [Q^2 + U^2]^{1/2}$$

and the degree, *P*, and position angle of polarization, *q*, using:

$$P = \frac{I_P}{I}$$

$$\theta = 28.648 \tan^{-1}\left(\frac{U}{Q}\right)$$

18.4.3 A Useful Script for Polarization Analysis

At the time of writing, we do not yet have NICMOS versions of all the IRAF software tools needed to solve these equations for our polarization images.

An interactive procedure to derive relevant parameters from NICMOS polarization images has been developed by Hines et al. (1997).[3] In addition to taking into account instrumental polarization, this routine corrects for flatfield uncertainties and for small shifts between the images.

However, first approximation results can be obtained with a straightforward IRAF script. The approach we follow here is the simplest possible path to determining the polarization properties from the data. It does not take into account the instrumental polarization and does not allow for systematic errors in the data. The script will yield the correct morphology but not the exact intensity of the polarization. There are more sophisticated tools available in the community, including the one referenced above, which have been developed specifically to analyze polarization images, and which will yield better results than this very simple approach. The IRAF script is included below, and is commented.

---

3. Hines, D.C., G.D. Schmidt, and D. Lytle, 1997, "The Polarimetric Capabilities of NICMOS," *HST Calibration Workshop*, S. Casertano et al. (eds.)

The script doesn’t take into account that in NIC1 the POL120 filter has only 48% transmission, while the POL0 filter has 98% transmission. For sake of simplicity, we assume here that the polarization image at 120 degrees has been obtained using the POL0 filter with a spacecraft roll, rather than using the POL120 filter.

Figure 18.4: Polarization Script

```
procedure pol( )
begin
!use `flpr’ to flush the process cache regularly to prevent IRAF !memory problems

!first generate the total intensity, pols_i
msarith(“pol0s”,”+”,”pol120s”,”tmp1”)
msarith(“tmp1”,”+”,”pol240s”,”tmp2”)
msarith(“tmp2”,”*”, 0.6666667,”pols_i”)
imdel(“tmp1”)
imdel(“tmp2”)
flpr

!now generate Stokes Q parameter, pols_q...
msarith(“pol0s”,”*”, 2.0, “tmp1”)
msarith(“tmp1”, “-”,”pol240s”,”tmp2”)
msarith(“tmp2”, “-”,”pol120s”,”tmp3”)
msarith(“tmp3”, “*”, 0.6666667,” pols_q”)
flpr
imdel(“tmp1”)
imdel(“tmp2”)
imdel(“tmp3”)
flpr

!...and next the Stokes’ U parameter, pols_u...
msarith(“pol240s”,”-”,”pol120s”, “tmp1”)
msarith(“tmp1”, “*”, 1.154701, “pols_u”)
imdel(“tmp1”)
flpr

!...now the polarized intensity...
msarith (“pols_q”,”*”,”pols_q”,”tmp1”)
msarith (“pols_u”,”*”,”pols_u”,”tmp2”)
msarith (“tmp1”, “+”,”tmp2”, “tmp3”)
flpr

!...this messy bit is to generate the uncertainty on the polarized !intensity...
imfunction(“tmp3”, “tmp4.fits”,”sqrt”)
imarith (“tmp3[2]”, “*”, 0.5, “tmp5.fits”)
!cp tmp3.fits pols_ip.fits
imcopy (“tmp4”,”pols_ip[1][1:256,1:256]”)
imcopy (“tmp5”,”pols_ip[2][1:256,1:256]”)
flpr
imdel(“tmp1”) imdel(“tmp2”) imdel(“tmp3”) imdel(“tmp4”) imdel(“tmp5”)
flpr

!...now here is the degree of polarization, pols_p...
msarith(“pols_ip”,”/”,”pols_i”,”pols_p”)

!...and finally, here comes the polarization angle, pols_theta...
msarith(“pols_u”,”/”,”pols_q”,”tmp1”)
flpr
imfunction(“tmp1”,”tmp2.fits”,”atan”)
!cp tmp1.fits pols_theta.fits
imarith (“tmp2”, “*”, 28.648, “tmp3.fits”)
flpr
imcopy (“tmp3”,”pols_theta[1][1:256,1:256]”)
imarith (“tmp1[2]”, “/”, “tmp1[1]”, “tmp4.fits”)
imarith (“pols_theta[1]”, “*”, “tmp4”, “tmp5.fits”)
flpr
imcopy (“tmp5”, “pols_theta[2][1:256,1:256]”)
imdel(“tmp1”)
imdel(“tmp2”)
imdel(“tmp3”)
imdel(“tmp4”)
imdel(“tmp5”)
flpr
end
```

The script assumes we started with three images, named `pol0s.fits`, `pol120s.fits` and `pol240s.fits`, taken in the short wavelength polarization filters. The output from the script is a set of files named `pols_u.fits` and `pols_q.fits` (the Stokes' U and Q parameters respectively), `pols_i.fits` (the total intensity), `pols_ip.fits` (the polarized intensity), `pols_p.fits` (the degree of polarization), and `pols_theta.fits` (the polarization angle). The error propagation should, in general, be more or less correct for statistical errors (all systematic errors are ignored), although for the polarization angle the error is a gross approximation. When a new version of the IRAF **imfunction** task is written to include error propagation, the rather messy parts of the above script which generate error arrays will no longer be needed.